Galaxies and Cosmology

Matthias Kadler

Wintersemester 2009/2010

Dr. Karl Remeis-Sternwarte, Bamberg & ECAP
matthias.kadler@sternwarte.uni-erlangen.de
Tel.: (0951) 95222-26

pulsar.sternwarte.uni-erlangen.de/wilms/teach/galcos_ws10

ERLANGEN CENTRE FOR ASTROPARTICLE PHYSICS

Friedrich–Alexander–Universität Erlangen–Nürnberg

Introduction

Contents: Galaxies

Introduction	
18 Oct	Organization; Stars and Galaxy
19 Oct	Galaxies, Evolution of the Universe
Local Group	
21 Oct	Members, Motions, ISM
02 Nov	ISM, Chemical Evolution
Spiral Galaxies	
08 Nov	Global Properties, Distribution of Gas
09 Nov	Density Wave Theory
15 Nov	Density Wave Theory, Bulges and Centers
Elliptical Galaxies	
22 Nov	Global Properties, Distribution of Matter
Active Galactic Nuclei	
29 Nov	Seyfert Galaxies, Black Hole Paradigm
30 Dec	Radio Loud AGN
Galaxy Clusters	
06 Dec	Galaxy Statistics, Interactions, Starbursts

Contents: Cosmology

Classical Cosmology	
13 Dec	Introduction, FRW
20 Dec	Distance Scale, H_0
21 Dec	Distance Scale, H_0
The Early Universe	
10 Jan	Hot Big Bang
17 Jan	Nucleosynthesis
18 Jan	Inflation
Properties of the Universe	
24 Jan	Measurement of Ω and Λ
25 Jan	Measurement of Λ
Structure Formation	
31 Jan	Measurement of Structure
07 Feb	EXAM
08 Feb	Structure Formation

Textbooks, I

Sparke & Gallagher, 2007, *Galaxies in the Universe – an Introduction*, Cambridge: CUP, 40.99 € (softcover)

Textbook for the 1st half of the class, somewhat lower level than what we will be teaching, but a very good overview nevertheless.

Binney & Merrifield, 1998, *Galactic Astronomy*, Princeton: Princeton University Press, 55 €, 791 pp.

Advanced level book on Galactic astronomy, the standard for graduate level courses, so higher than what we will be doing, but a very good book if you want to continue to do astronomy. Recommended.

Schneider, P., 2005, *Einführung in die Extragalaktische Astronomie und Kosmologie*, Heidelberg: Springer, 59.95 € (available as an e-book)

Well written introduction to cosmology, approximately at the level of this lecture. Recommended.

Textbooks, II

Peacock, J.A., 1999, *Cosmological Physics*, Cambridge: Cambridge Univ. Press, 49.50 €

Very exhaustive, but difficult to read since the entropy per page is *very* high. . . still: a "must buy".

Longair, M.S., 1998, *Galaxy Formation*, Berlin: Springer, 53.45 €

Clear and pedagogical treatment of structure formation.

Carroll & Ostlie, 2007, *Modern Astrophysics*, Reading: Addison-Wesley, 80 €(softcover), 1400 pp.

Advanced level, expects good physics background, generally I like their stellar astrophysics part better than their extragalactic one.

Exercises and Exam

We will have 2 h long exercise sessions led by Thomas Dauser and Tobias Beuchert approximately every 2 weeks at the following dates:

28 Oct	Milky Way
18 Nov	Spiral Galaxies
25 Nov	ADS, NED, Simbad, Proposals
09 Dec	AGN
16 Dec	1st Iteration Proposals / World Models
23 Dec	Proposal Email Submission Deadline
13 Jan	Observing Panel
03 Feb	1 h Test Exam

Note that your presence at the exercise sessions is mandatory

(unless you have a lab experiment)

In general, exercises are "in class" (i.e., no homeworks).

We will also give out reading assignments and other exercises to help you with the course.

Exercises and Exam

In addition to standard practicals, we will go through an "observing proposal" exercise, where you will

. . . write (alone or with a partner) a one-page scientific justification for an astronomical observation

. . . discuss a preliminary draft with one of us

. . . read $\sim$ 5 proposals written by your colleagues, present and discuss them in an "observing panel"

. . . rank proposals by scientific importance.

Overview

Optical View of B68 (ESO; VLT/FORS1)

Introduction

Galaxies and the universe consist of stars, and basic knowledge on the properties of stars and of Galaxies is required.

Before starting with this course, we will therefore briefly review the most important properties of stars, the Milky Way, Galaxies and the Universe, to bring everybody up to speed.

For details please consult lecture notes for “Introduction to Astronomy” at
`http://pulsar.sternwarte.uni-erlangen.de/wilms/teach/intro`

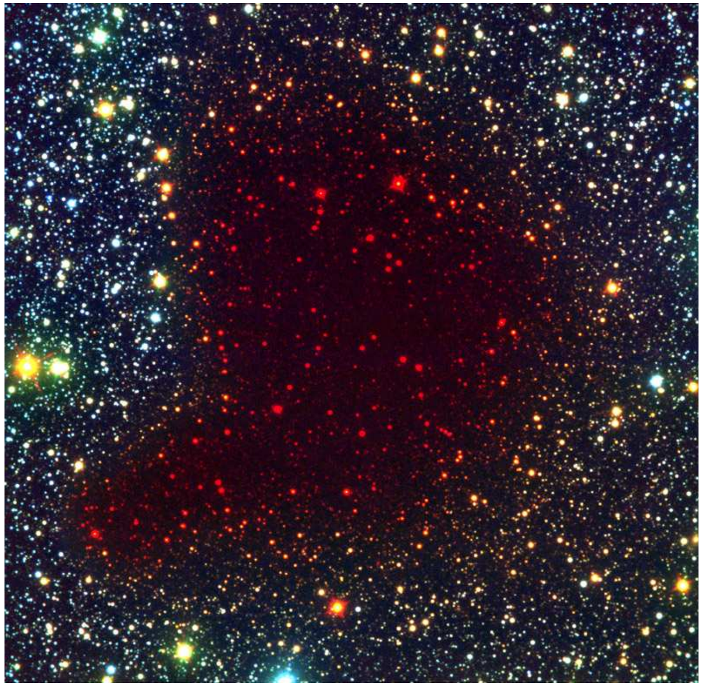

IR View of B68 (ESO; VLT/FORS1 + NTT/SOFI)

Formation

Stars are born in "Giant Molecular Clouds"

Typical GMC parameters (e.g., Orion):

- large clouds: typical diameters 50–100 pc
- contain lots of molecular gas (H_2, CO, alcohol,...).
- typical temperatures: 10–20 K (coolest regions in the interstellar medium)
- typical particle densities $n \sim 10^6$–$10^{10}\,\mathrm{cm}^{-3}$

Stars are born in groups out of collapsing Molecular Clouds.

Collapse triggered, e.g., by collisions of clouds or shocks caused by nearby supernovae.

Formation

Criterion for collapse: Cloud is instable, i.e., gravitation is stronger than thermal pressure.

In terms of thermal and gravitational energies, this means

$$\frac{3}{2}\frac{M}{m_\mathrm{p}}kT - \frac{3}{5}\frac{GM^2}{R} \leq 0 \tag{2.1}$$

which can be expressed as

$$\frac{M}{R} \geq \frac{5}{2}\frac{kT}{Gm_\mathrm{p}} \quad \text{or} \quad \frac{4\pi}{3}\rho R^2 \geq \frac{5}{2}\frac{kT}{Gm_\mathrm{p}} \tag{2.2}$$

$\Longrightarrow$ Depends on R, collapse thus possible for

$$R > R_\mathrm{J} = \sqrt{\frac{15kT}{8\pi G m_\mathrm{p}\rho}} \sim \sqrt{\frac{kT}{G m_\mathrm{p}\rho}} \tag{2.3}$$

where R_J is called the Jeans radius.

Formation

Plugging in typical typical numbers, i.e., $T \sim 50\,\mathrm{K}$, particle density $n = 10^5$ H-atoms cm^{-3} (=a mass density of $\rho = nm_\mathrm{p} \sim 1.7 \times 10^{-9}\,\mathrm{g\,cm}^{-3}$) gives $R_\mathrm{J} \sim 0.2\,\mathrm{pc}$.

For a given Jeans radius, the mass within R_J is the Jeans mass

$$M_\mathrm{J} \sim \frac{4\pi}{3}R_\mathrm{J}^3\rho \tag{2.4}$$

...which has typical values of 50–100 $M_\odot$, i.e., larger than one star!

In reality things are more complicated: ISM contains magnetic fields

$\Longrightarrow$ Particle motion $\perp$ B-field lines difficult

$\Longrightarrow$ stops gas from collapsing.

This is good since Jeans formalism alone predicts too strong star formation.

$\Longrightarrow$ Need star formation with magnetic fields

See Shu et al. (1987, Annual Reviews of Astronomy and Astrophysics 25, 23) for the gory details.

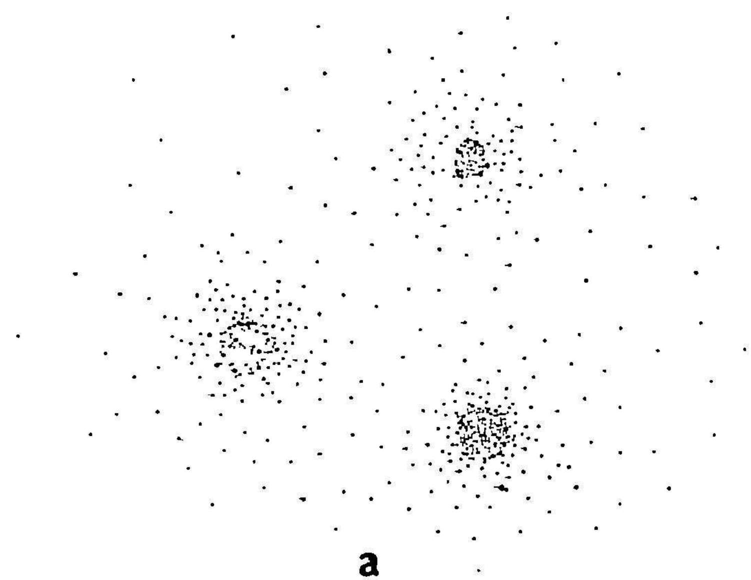

Shu et al. (1987, ARAA 25, 23, Fig. 7)

Stellar mass cores form from fragmentation of larger pieces.

Note: fragmentation only along B-field lines.

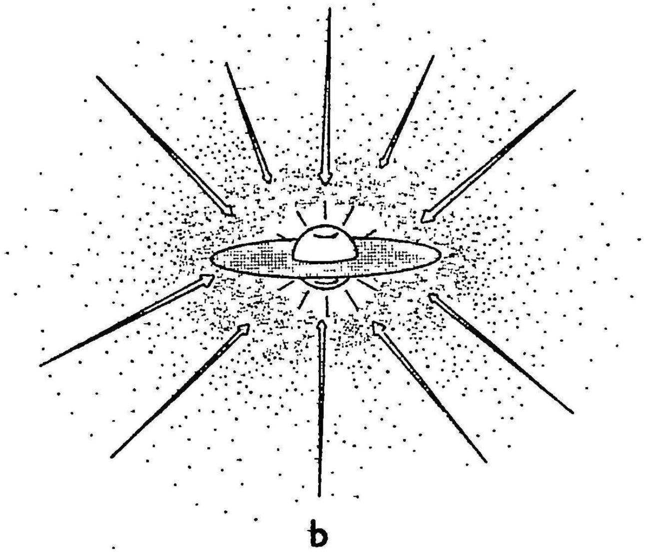

Shu et al. (1987, ARAA 25, 23, Fig. 7)

Protostar forms with surrounding disk ("inside out collapse") once core hot enough to allow fusion ($T > 10^6$ K)

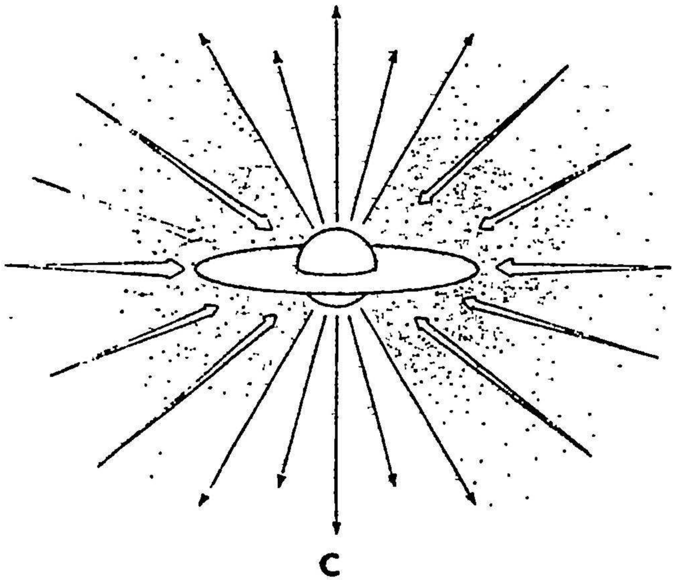

Shu et al. (1987, ARAA 25, 23, Fig. 7)

Stellar wind forms bipolar outflow

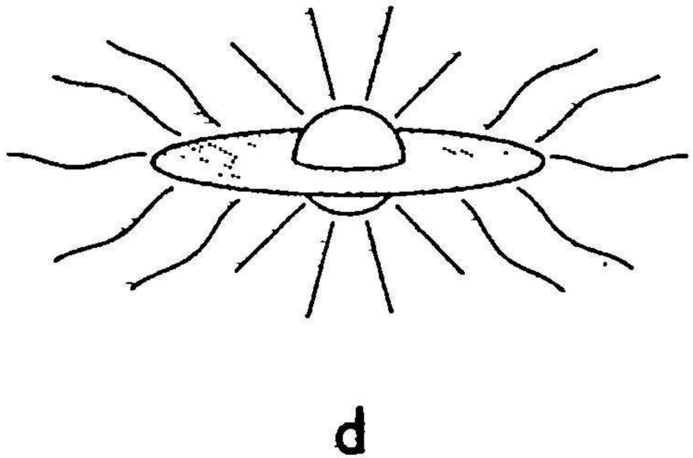

Shu et al. (1987, ARAA 25, 23, Fig. 7)

Star has reached zero age main sequence (ZAMS) plus circumstellar disk. Some disks produce fast collimated outflows (jets): Herbig Haro Objects

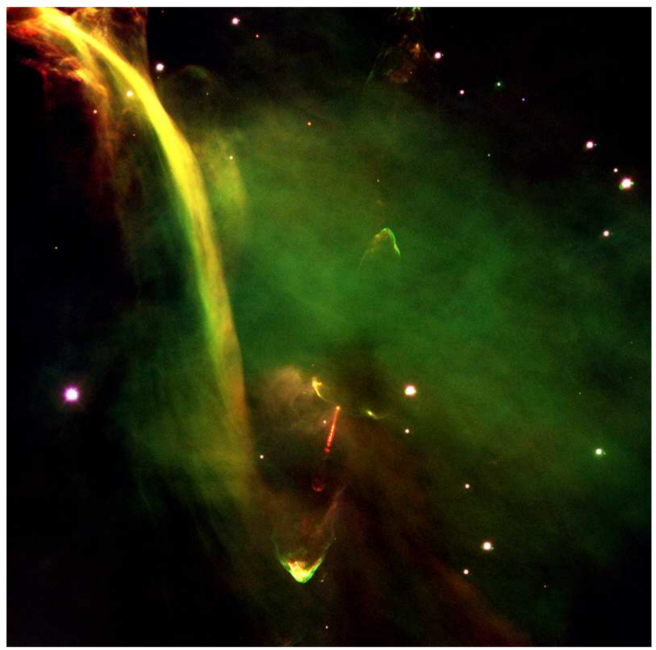

HH34 in Orion (ESO VLT KUEYEN/FORS2)

Herbig Haro Objects: shocks and jets/outflows produced during formation of stars.

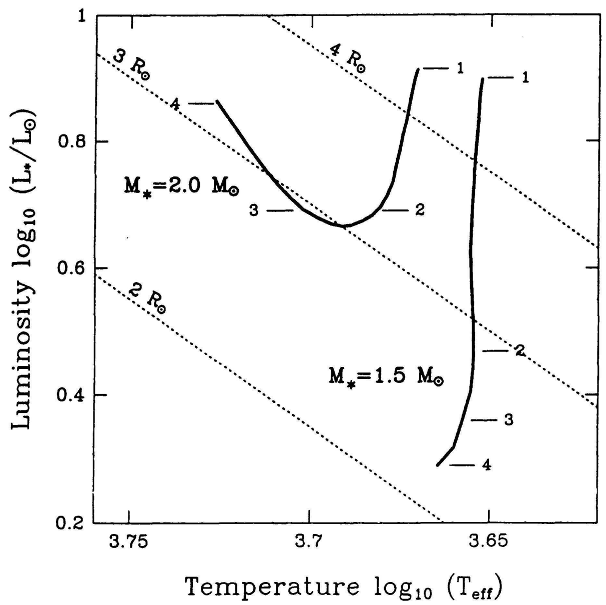

Palla & Stahler (1993, ApJ 418, 414; numbers are time in 10^6 years)

Stellar Evolution from protostar to ZAMS takes a few million years.

Zero Age Main Sequence, II

Once star has collapsed and nuclear fusion has started: zero age main sequence (ZAMS) is reached

The Main Sequence is the result of steady state fusion ("burning") of hydrogen into helium in stellar centers.

. . . longest phase of stellar evolution (10 billion years for Sun)

Stellar structure defined by balance between pressure inwards due to gravitation and pressure outwards due to energy release ("hydrostatic equilibrium").

Zero Age Main Sequence, III

The structure of stars is defined by a set of four coupled differential equations which express the basic conservation and transport quantities always encountered in physics:

1. Mass conservation
2. Momentum conservation (=hydrostatic equilibrium)
3. Energy conservation
4. Energy transport

and quantities expressing the physical properties of material, mainly:

1. Energy generation
2. Equation of state (=dependence of density of material from physical conditions)

Zero Age Main Sequence, IV

Stellar structure governed by four coupled differential equations:

Mass structure
(mass conservation)

$$\frac{\mathrm{d}M}{\mathrm{d}r} = 4\pi r^2 \rho(r)$$

Pressure structure
(hydrostatic equilibrium)

$$\frac{\mathrm{d}P}{\mathrm{d}r} = -\rho(r)\frac{GM(r)}{r^2}$$

Temperature structure
(e.g. radiative transfer)

$$\frac{\mathrm{d}T}{\mathrm{d}r} = -\frac{3}{4ac}\frac{\kappa\rho(r)}{T^3}\frac{L(r)}{4\pi r^2}$$

Energy conservation

$$\frac{\mathrm{d}L}{\mathrm{d}r} = 4\pi r^2 \rho(r)\epsilon(r)$$

plus "equation of state" ($P = P(T, \rho)$), Opacities $\kappa(T, \rho, Z)$ = interaction of radiation with gas, energy generation ($\epsilon = \epsilon(T, \rho, Z)$),. . .

Stellar model: numerical solution of stellar structure equations.

Energy generation: Overview

Main sequence: Nuclear fusion of Hydrogen into Helium:

$$4\text{p} \longrightarrow {}^4_2\text{He} + E$$

How much energy is gained?

Particle physics: express mass as "rest energy equivalent" via $E = mc^2$

(and call it "mass"...); usually use energy units of MeV, 1 MeV $= 1.602 \times 10^{-13}$ J

	mass of 4 protons (4×938 MeV):	3752 MeV
−	mass of ${}^4_2$He:	3727 MeV
	mass defect Δmc^2:	25 MeV

In the fusion of hydrogen to helium, 0.7% of the available rest mass energy is converted to energy.

Two main burning cycles: proton-proton chain and the CNO cycle.

Energy generation: Proton-Proton chain

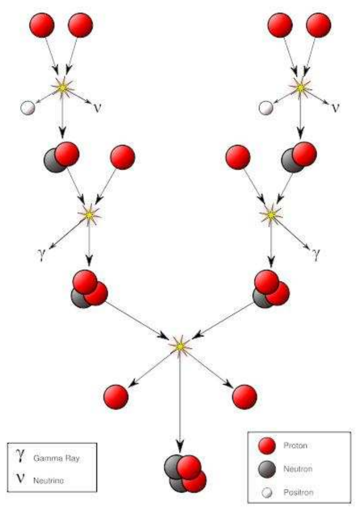

For moderate central temperatures, He is produced using the proton proton chain.

First, two protons create a deuteron:

$${}^1\text{H} + {}^1\text{H} \longrightarrow {}^2\text{H} + \text{e}^+ + \nu_\text{e} \tag{2.5}$$

This process is slow (happens once for a nucleon per 10^{10} years)

Then an additional proton is attached:

$${}^2\text{H} + {}^1\text{H} \longrightarrow {}^3\text{He} + \gamma \tag{2.6}$$

and two helium nuclei can form an alpha particle:

$${}^3\text{He} + {}^3\text{He} \longrightarrow {}^4\text{He} + 2\,{}^1\text{H} \tag{2.7}$$

This is the so called pp I-cycle, minor variations of the theme exist (pp II, pp III cycles), but pp I dominates.

pp chain dominates for $T \lesssim 2 \times 10^7$ K, $\epsilon_\text{pp} \propto T^5$;

Sun: 98.4%.

Energy generation: CNO cycle

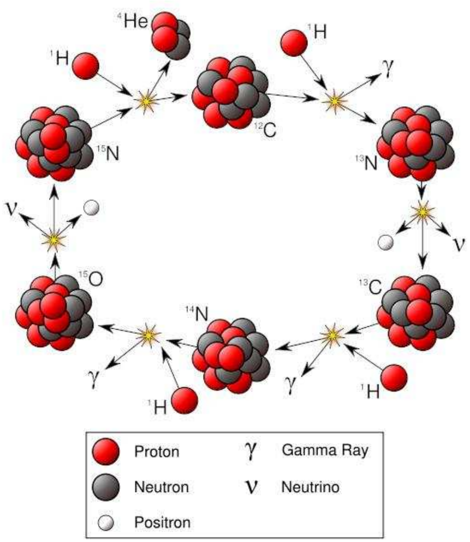

The CNO cycle (Bethe-Weizsäcker-cycle) requires the presence of C, N, and O isotopes as catalysts.

CNO cycle has slightly smaller energy release than pp-cycle because of higher neutrino losses.

Reaction ${}^{14}\text{N} + \text{p} \longrightarrow {}^{15}\text{O} + \gamma$ is th slowest reaction (one million years).

CNO cycle dominates above 2×10^7 K, $\epsilon_\text{CNO} \propto T^{17}$;

Sun: 1.6%.

Wikipedia

Characteristic Timescales

Main sequence: Hydrogen burning at the center.

Evolution timescale dominated by the nuclear timescale = timescale needed to use the fuel in the center of the star.

According to simulations, this is ∼10% of the available Hydrogen.

Since 0.7% of $M_\text{core}c^2$ converted into He, the nuclear timescale is

$$t_\text{n} = \frac{0.007 \cdot 0.1 Mc^2}{L} = \frac{M/M_\odot}{L/L_\odot} \cdot 10^{10}\,\text{years} \tag{2.8}$$

A second important timescale is the timescale the star would need to radiate its stored thermal energy: thermal timescale.

Roughly given as

$$t_\text{t} = \frac{0.5GM^2/R}{L} = \frac{(M/M_\odot)^2}{(R/R_\odot)(L/L_\odot)} \cdot 2 \times 10^7\,\text{years} \tag{2.9}$$

Internal Structure

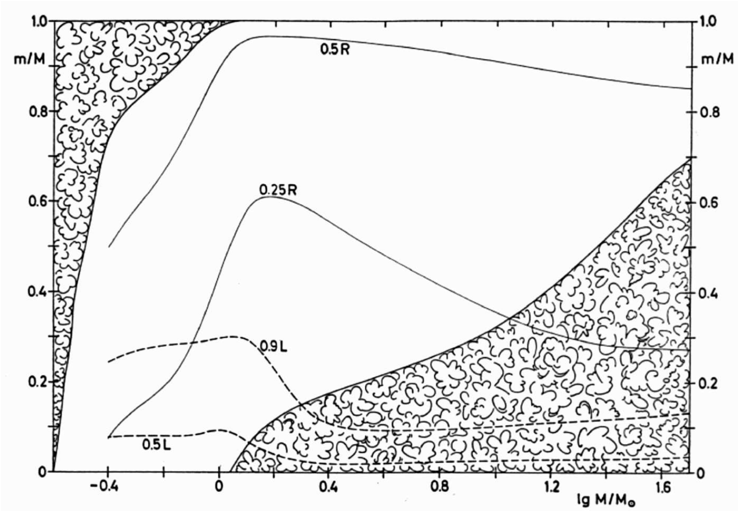

Kippenhahn diagram: Internal Structure of Main Sequence stars

Evolution on the Main Sequence

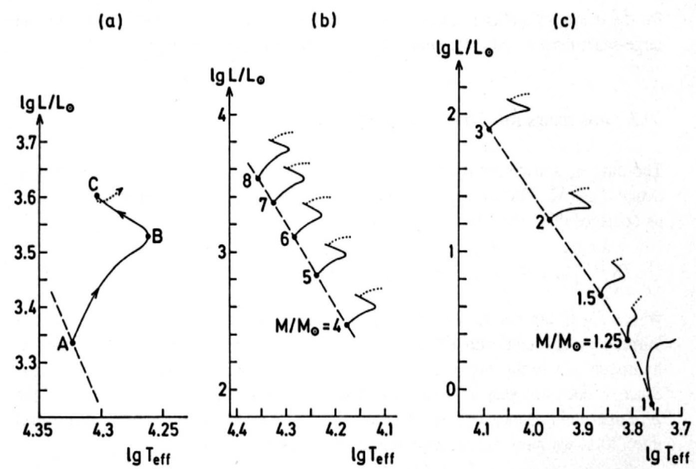

main sequence evolution from zero age to helium exhaustion

Evolution: Low Mass Stars, I

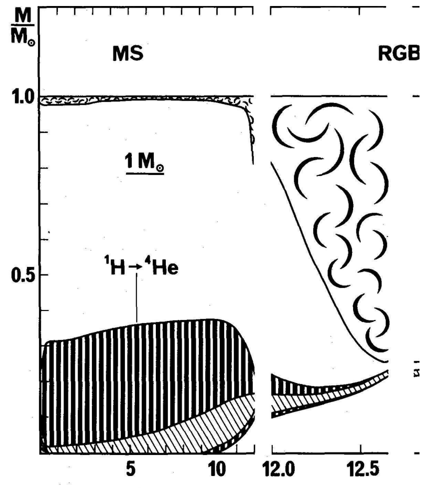

(Maeder & Meynet, 1989)

Once H is exhausted in center: H continues to burn in a shell around the He core ("shell burning").

For stars with $M \lesssim 1\,M_\odot$: Star reacts by expanding convective hull until it is almost fully convective.

Evolution: Low Mass Stars, II

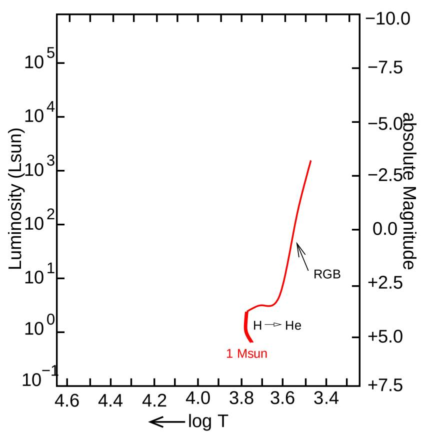

(after Iben, 1991)

Once H is exhausted in center: H continues to burn in a shell around the He core ("shell burning").

For stars with $M \lesssim 1\,M_\odot$: Star reacts by expanding convective hull until it is almost fully convective.

$\Longrightarrow$ luminosity increases, temperature decreases

$\Longrightarrow$ motion in HRD horizontally towards the right, then upwards to higher L: red giant stage.

Evolution: Low Mass Stars, III

After H-burning, note that stars are in hydrostatic equilibrium: inwards gravitational pressure balanced by outwards gas pressure

Note: gas pressure, emphnot radiation pressure!

Since the gas pressure is $P = nkT$: energy source needed to heat gas (=fusion).

This is a problem for the core during the red giant stage, as virtually no fusion ongoing

$\Longrightarrow$ Core gets compressed

$\Longrightarrow$ ρ and T increase

BUT: collapse cannot continue indefinitely!

$\Longrightarrow$ once ρ has increased appreciably, there must be a point where the Pauli principle becomes important: stellar matter degenerates, resulting in $P \propto \rho^{5/3}$ (independent of T!)

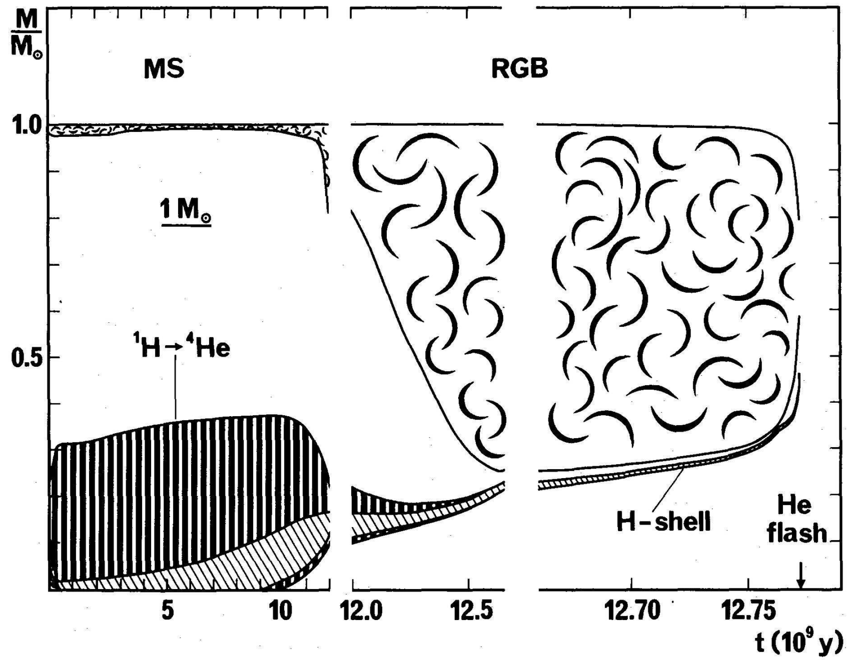

Evolution of the structure of a 1 $M_\odot$ star to the Helium flash (Maeder & Meynet, 1989).

Evolution: Low Mass Stars, IV

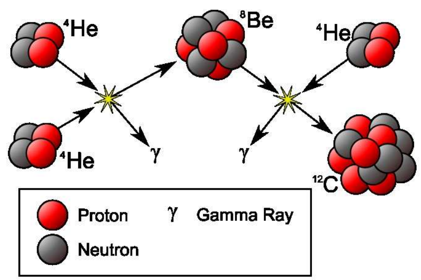

In the degenerate core, once $T_{\text{core}} \sim 100 \times 10^6$ K: Triple alpha process starts:

$$^4\text{He} + {}^4\text{He} \leftrightarrow {}^8\text{Be}$$
$$^8\text{Be} + {}^4\text{He} \rightarrow {}^{12}\text{C}$$

Since ^{8}Be has a half life of only 2.6×10^{-16} s: this can only work effectively if 3 α-particles collide.

But core is degenerate:

$\Longrightarrow$ High thermal conductivity of electrons

$\Longrightarrow$ core has uniform temperature

$\Longrightarrow$ 3α onset is rapid

$\Longrightarrow$ He flash

Not seen on surface ("buffered" by convective envelope).

Evolution: Low Mass Stars, VI

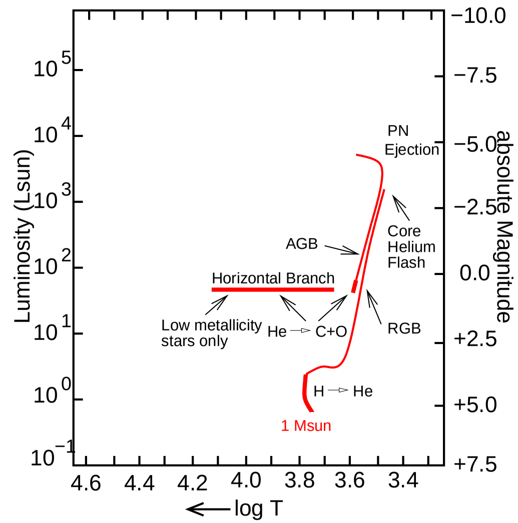

After the He flash, He burning in core and H shell burning

$\Longrightarrow$ expansion starts again

$\Longrightarrow$ "asymptotic giant branch"

Unstable He fusion processes ("thermal pulses") lead to ejection of outer layers (~50% of total mass!)

Effect of He core being unable to transport energy away quickly enough.

$\Longrightarrow$ inner (hotter) parts of star become visible.

after Iben (1991)

Evolution: Low Mass Stars, VII

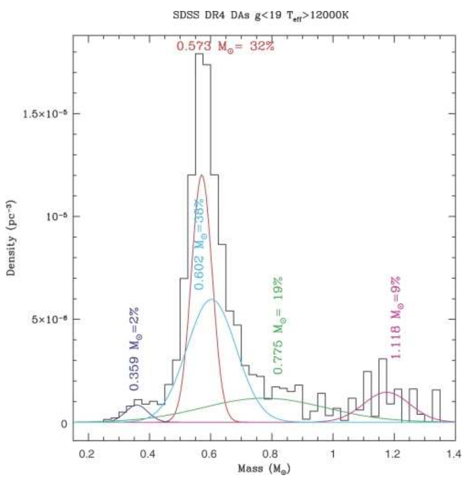

mass distribution of 1733 white dwarfs (Kepler et al. 2007, MNRAS 375, 1315)

White Dwarfs

1. End stages of evolution of stars born with $M \lesssim 8\,M_\odot$
2. mainly consist of C and O
3. Radius $\sim$ Earth
4. typical density $\rho \sim 10^6\,\mathrm{g\,cm^{-3}}$
5. typically $M \sim 0.6 M_\odot$
   $M < 1.44\,M_\odot$ (Chandrasekhar mass); above that: relativistic degenerate gas ($P \propto \rho^{4/3}$), can show that under these circumstances WD is not stable.

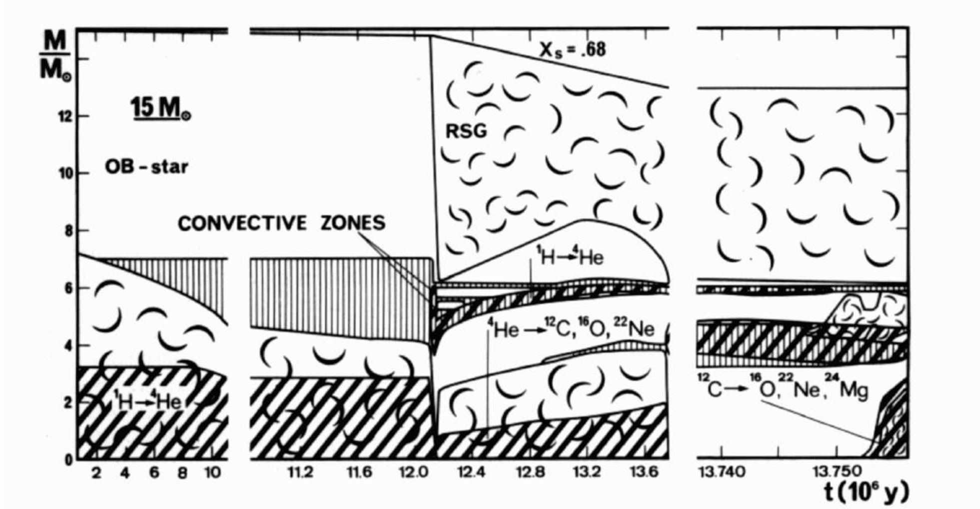

Evolution of the internal structure of a 15 $M_\odot$ star.

Massive Stars

Massive stars: Evolution on MS similar but faster than for low mass stars.

More massive stars reach threshold temperature for 3α and subsequent nuclear burning before reaching degeneracy

$\Longrightarrow$ He just starts to burn.

In these objects, higher order fusion processes can kick in (but are energetically unimportant): alpha reactions

$$^{12}\mathrm{C} + {}^{4}\mathrm{He} \rightarrow {}^{16}\mathrm{O} + \gamma$$
$$^{16}\mathrm{O} + {}^{4}\mathrm{He} \rightarrow {}^{20}\mathrm{Ne} + \gamma$$
$$^{20}\mathrm{Ne} + {}^{4}\mathrm{He} \rightarrow {}^{24}\mathrm{Mg} + \gamma$$

Outer layers continue H shell burning.

During evolution of star on red giant branch: convective hull moves deeper into core, can mix fusion products into outer layers.

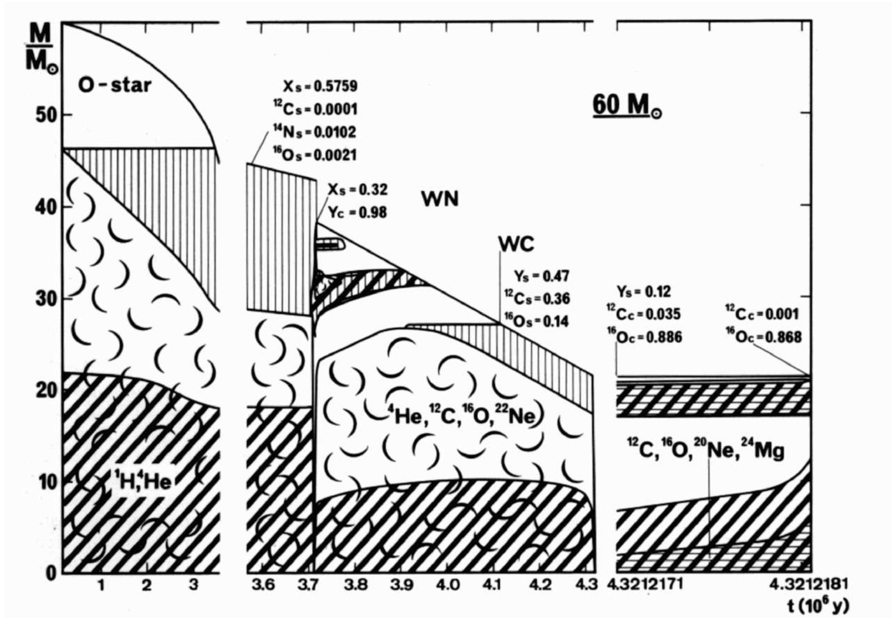

Evolution of the internal structure of a 60 $M_\odot$ star.
Note the very strong mass loss!

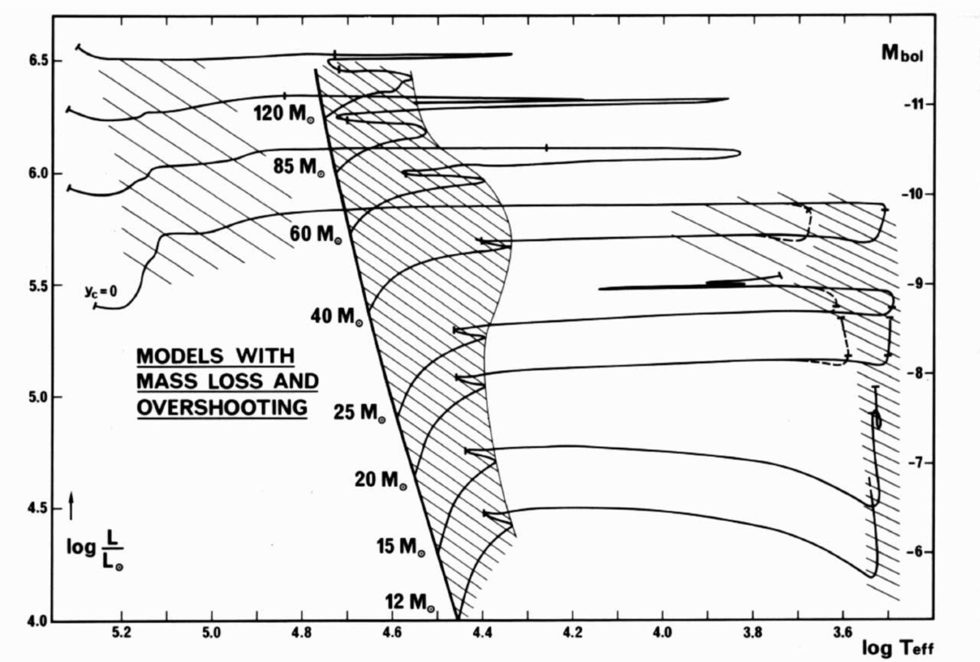

Summary: Evolution of massive stars in the HRD.

Massive Stars

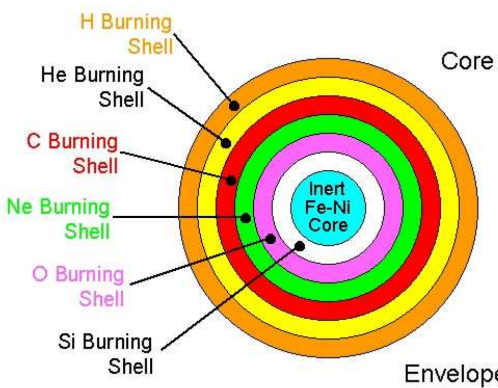

Core Radius: ~1 R_{earth}

Envelope Radius: ~ 5 AU

successive stages of nuclear burning: final state: onion-shell model

1. H burning, ash: He
2. He burning, ashes: C, O, Ne, Mg
3. C burning, ashes: Ne, Na, Mg
4. Ne burning, ashes: O, Mg . . .
5. O burning, ashes: Si, P, S, . . .
6. Si burning, ashes: Fe, Ni

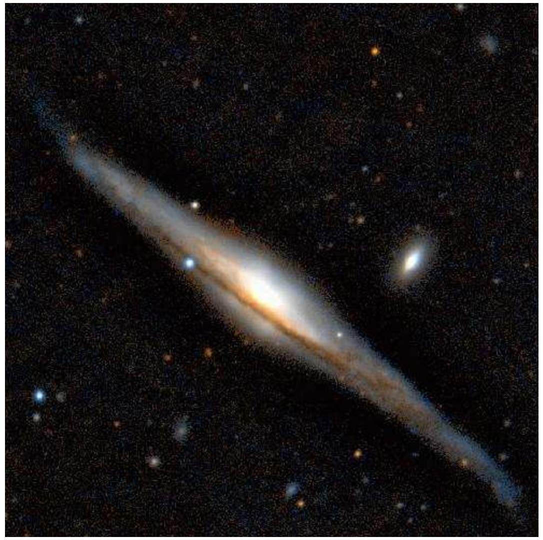

Type II SN2001cm in NGC5965 (2.56 m NOT, Håkon Dahle; NORDITA)

Evolution of more massive stars: fusion up to ^{56}Fe, then no energy gain $\Longrightarrow$ no pressure balance in centre $\Longrightarrow$ supernova explosion of type II.
energy release: 10^{46} W ($10^{20} L_\odot$; about 1% in light, rest in neutrinos)

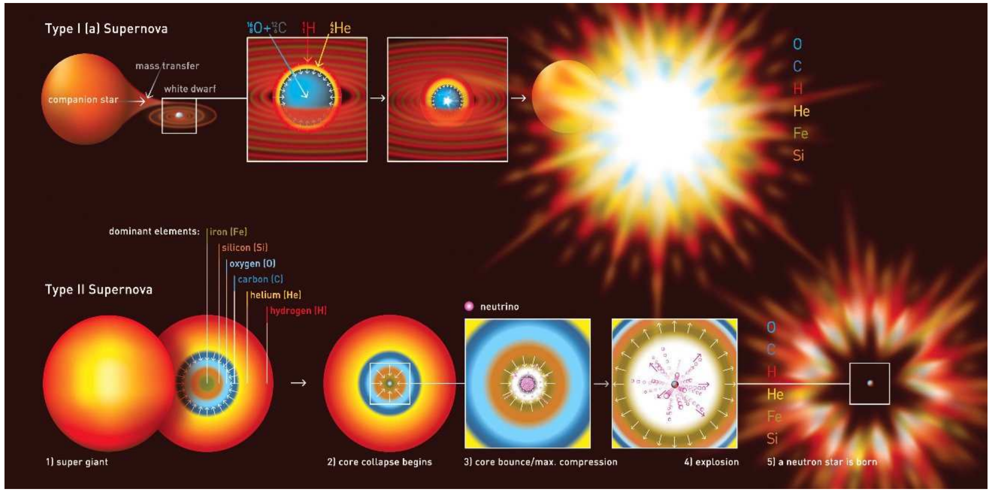

F.K. Thielemann

Outcome: Neutron Stars or Black Holes

Structure of the Galaxy, I

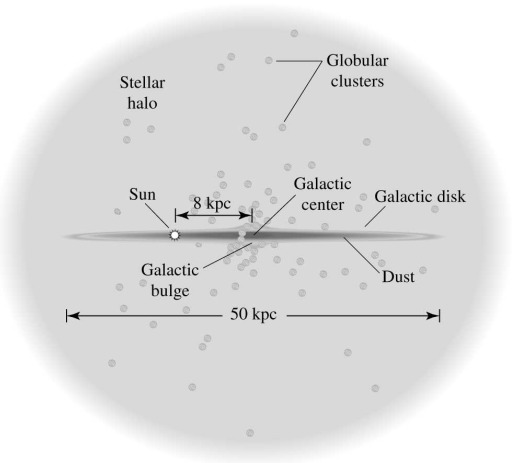

components of the Milky Way:

- Galactic disk:
  - rotating
  - young & old stars, open star clusters
  - gas & dust
- Galactic halo:
  - non-rotating,
  - old stars only, globular clusters
  - no gas, no dust
- Galactic bulge: rigid rotation

Structure of the Galaxy, II

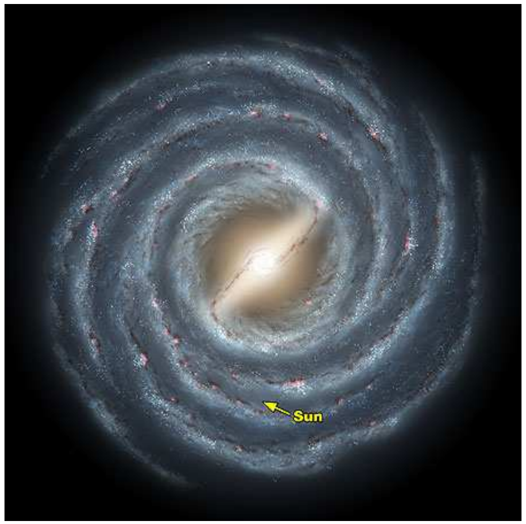

Milkyway is a barred spiral galaxy Luminosity:
$\sim 2 \times 10^{10}\,L_\odot$
Mass: $\sim 10^{11}\,M_\odot$ (radiating)
$\sim 10^{12}\,M_\odot$ (total)
Stellar density: $\sim 0.3\,M_\odot\,\mathrm{pc}^{-3}$

$1\,M_\odot = 2\times 10^{33}\,\mathrm{g} = 2\times 10^{30}\,\mathrm{kg}$,
$1\,L_\odot = 4\times 10^{33}\,\mathrm{erg\,s^{-1}} = 4\times 10^{26}\,\mathrm{W}$

Evidence for Spiral Arms

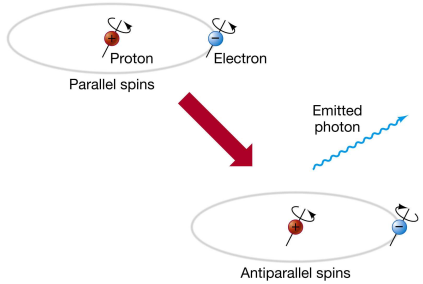

Image: 2005, Pearson Prentice Hall, Inc.

- Spins of electron and proton may be parallel ($F = 1$) or antiparallel ($F = 0$) ("hyperfine levels"); energy difference of $\Delta E \sim 6 \times 10^{-6}$ eV, corresponding to $\lambda = 21$ cm or $\nu = 1.4$ GHz.
- $F = 1$ is metastable, i.e., long life time (10^7 years); transition to $F = 0$ *dipole forbidden* in quantum mechanics, transition rate 10^{-6} smaller than for permitted transitions.
- Laboratory: $F = 1$ state is depopulated by collisions; no line is seen.
- ISM: low densities, i.e., no collisions; radiative transitions possible.

Because of the ubiquity of hydrogen, 21 cm line traces gas extremely well. Self-absorption of the line is extremely unlikely $\Longrightarrow$ line visible from everywhere except for the most dense regions.

Evidence for Spiral Arms

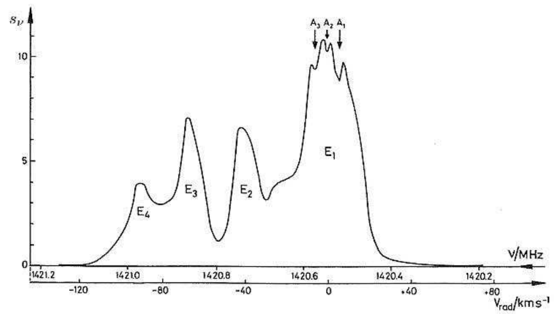

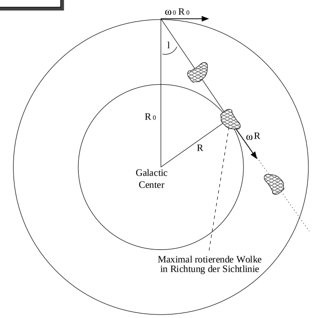

Sketch of a typical H I emission line profile. Note: v-axis has wrong sign!

In general multiple hydrogen clouds along the line of sight. Differential rotation ⇒ Differential Doppler shift, allows to obtain $\Omega(R)$ (note: maximum v_r at $R = R_0 \sin \ell$!).

Overall: Probe of ISM structure and dynamics!

Integration over the full profile gives the column density of neutral hydrogen in this direction. Typical values: $10^{18}\,\mathrm{cm}^{-2}$ (at large gal. latitudes) to $10^{22}\,\mathrm{cm}^{-2}$ (in the gal. plane).

State of the art is the Leiden-Argentine-Bonn Survey (Kalberla et al., 2005).

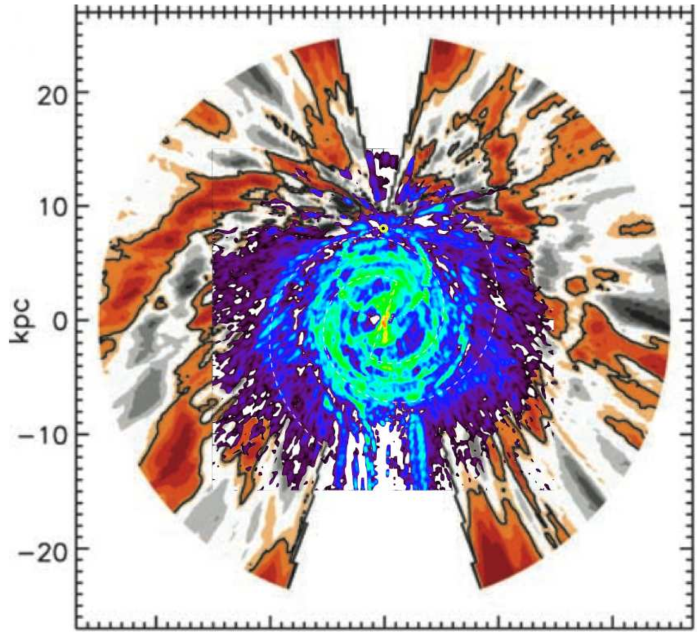

from Englmaier, Pohl, Bissanz (2008, Fig. 2; Sun is yellow dot)

Distribution of CO and H gas shows clearly the spiral structure.

Evidence for Spiral Arms

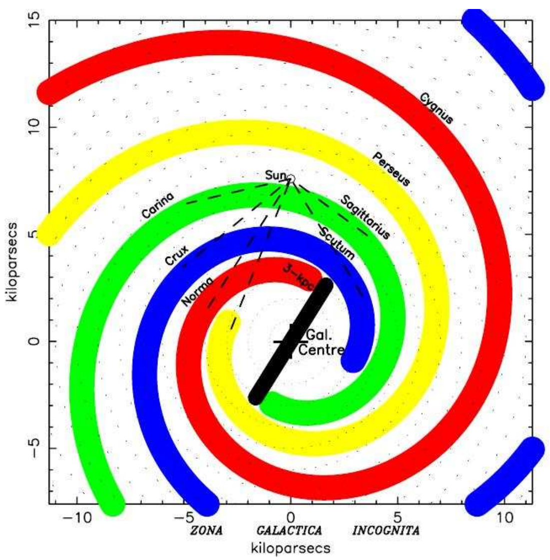

The spiral arm structure of Galaxy is now rather well understood

Vallee (2008)

Classification, I

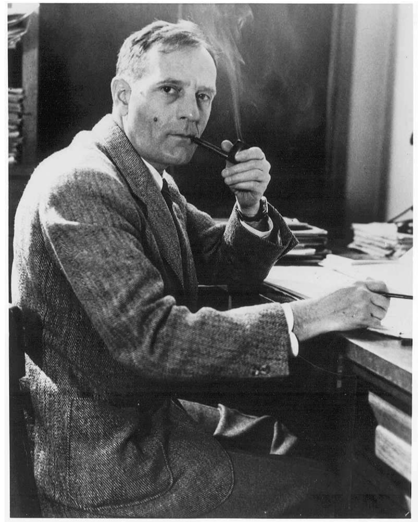

1920s: Hubble and others: classification of galaxies

- Morphology: Appearance on photographs, photographic emulsion is blue sensitive
- *Warning:* scheme is in parts not so well defined, incomplete, and not unique
- Note: photometric (colors) and spectroscopic information are not part of the Hubble scheme.

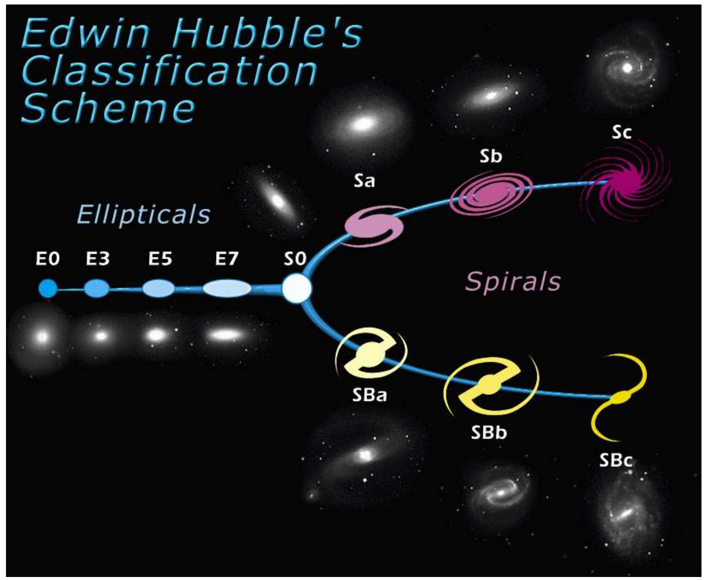

SDSS

Galaxy classification via the Hubble “tuning fork diagram”: “early types”: elliptical galaxies; “late types”: spiral galaxies, Not an evolutionary sequence!

Classification, III

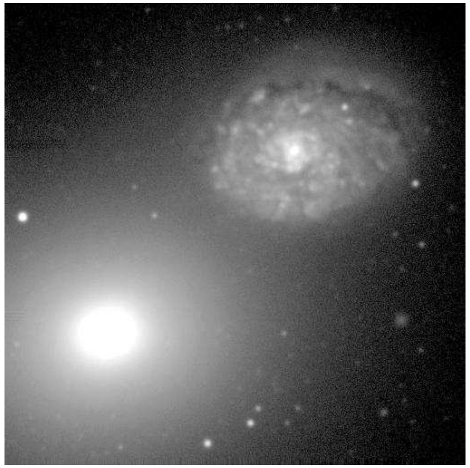

M60 (NGC 4649), E1, U. of Alabama

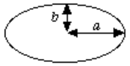

Elliptical galaxies: Classification as Ex where $x = 10(a-b)/a$ (integer part; between 0 and 7)

Ellipticals are low on dust and gas, reddish color (=old stars!), typically low luminosity and low mass ($10^6\,M_\odot$)

Monsters: Also elliptical, from mergers in galaxy clusters (e.g., M87 in Virgo), M up to $10^{12}\,M_\odot$, designated cD.

Barred Spirals

M95 (NGC 3351), SBb, INT

Barred Galaxies: Classification as SBa, SBb, SBc similar to Sx galaxies, but additional presence of a bar (cause of bar production and stability are still debated).

Similar masses and gas content as in normal spirals.

Milky Way is a barred spiral.

Spiral Galaxies

M51 (NGC 5194 and 5195), Sc and Irr, Kitt Peak 0.9 m

Spiral Galaxies: Elliptical nucleus ("bulge") plus disk with spiral arms, designated Sa, Sb, Sc depending on opening angle of spiral (Sa: $\sim 10^\circ$, Sc: $\sim 20^\circ$) and dominance of nucleus.

Bluer than ellipticals.

Mass content $\sim 3\times 10^{11}\,M_\odot$, with $M/L \sim 20$,

Gas content increases from Sa to Sc from 1% to 8%.

Spiral arms probably due to density wave.

Expansion of the Universe

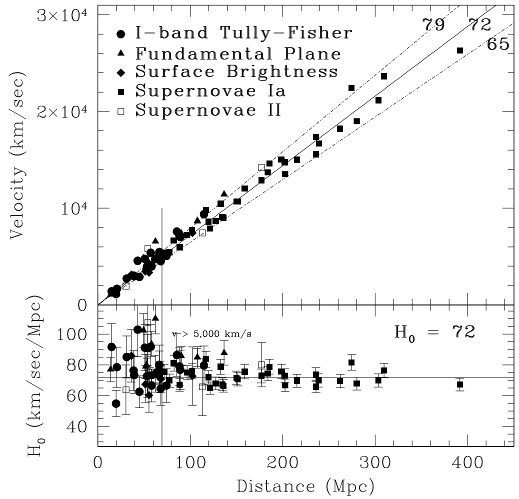

(Freedman, 2001, Fig.4)

Hubble relation (1929):

The redshift of a galaxy is proportional to its distance: $v = cz = H_0 d$

where H_0: "Hubble constant".
Measurement: determine v from redshift (easy), d with standard candles (difficult)
$\Longrightarrow H_0$ from linear regression.
Hubble Space Telescope finds

$H_0 = 72 \pm 8\,\mathrm{km\,s^{-1}\,Mpc^{-1}}$

CMB, I

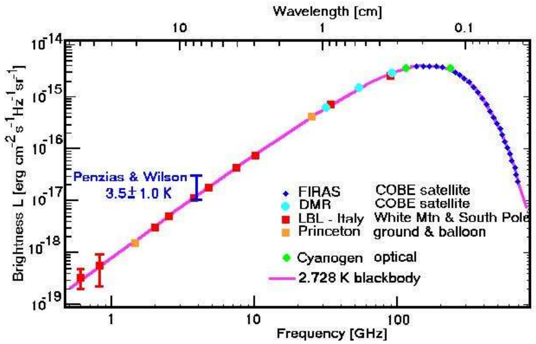

There is a cosmic microwave background (CMB), which is a perfect black body with $T = 2.725 \pm 0.002$ K

$\Longrightarrow$ Universe started hot, then temperature decreased as universe expanded,

$$T(z) = T_0(1+z) \qquad (2.10)$$

CMB, II

$a(t)$	t since BB	T[K] [K]	ρ_{matter} [g cm^{-3}]	Major Events
	10^{-42}	10^{30}		Planck era, "begin of physics"
	$10^{-40\ldots-30}$	10^{25}		Inflation?
10^{-13}	$\sim 10^{-5}$ s	$\sim 10^{13}$	$\sim 10^{9}$	generation of p-p^{-}, and baryon anti-baryon pairs from radiation background
3×10^{-9}	1 min	10^{10}	0.03	generation of e^{+}-e^{-} pairs out of radiation background
10^{-9}	10 min	3×10^{9}	10^{-3}	nucleosynthesis
$10^{-4}\ldots10^{-3}$	$10^{6\ldots7}$ yr	$10^{3\ldots4}$	$10^{-21\ldots-18}$	End of radiation dominated epoch
7×10^{-4}	10^{7} yr	4000	10^{-20}	Hydrogen recombines, decoupling of matter and radiation
			Formation of structures	
1	15×10^{9} yr	3	10^{-30}	now

General structure formation

General idea of all theories of structure formation:

1. Big Bang generates initial density perturbations (=potential wells)
   density perturbations caused by Poisson statistics in the early universe, e.g., decay of inflaton or similar
2. Those density fluctuations that can grow, grow.
3. Those density fluctuations that cannot grow get smoothed out by expansion and disappear.

How fluctuations grow depends on properties of material forming structures:

Early theory (Zeldovich, 1960s): structures=baryons; large structures must form first $\Longrightarrow$ this is not what is observed.

New theory: dark matter is important:

1. DM forms initial potential wells
2. Wells develop as universe expands
3. Baryons fall into potential wells once radiation and matter decouple
4. galaxies formed first, clusters still forming

Dark Matter

Detailed theory of structure formation uses numerical simulations, using CMB boundary conditions and assumptions on dark matter:

Hot Dark Matter: relativistic particles (e.g., neutrinos): moving with $v \sim c$. Fast particles

$\Longrightarrow$ smears out small density perturbations

$\Longrightarrow$ "top down structure formation"

Not what is observed

(observed: galaxies were there first, clusters are still forming)

Cold Dark Matter: slow particles, condense first, forming potential wells while baryonic matter is still coupled to radiation.

Once radiation decouples from matter (when universe is cold enough), matter falls in gravity wells.

$\Longrightarrow$ "bottom up structure formation"

Closer to what is observed

Luminous baryonic mass traces Dark Matter

Dark Matter

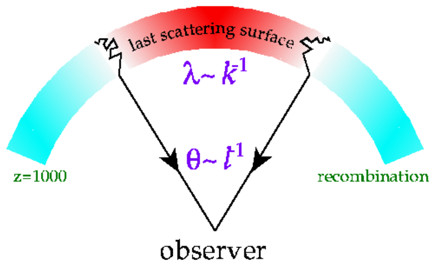

courtesy Wayne Hu

After BB: Universe is dense (“forry”), photons scatter efficiently off electrons ⟹ coupling of matter and radiation

Universe cools: recombination of protons and electrons to form hydrogen
⟹ no free electrons
⟹ no scattering
⟹ photons stream freelty

Photons leaving overdense regions loose energy (gravitational red shift)
⟹ visible as a temperature fluctuation (Sachs-Wolfe-Effect)

Leads to CMB fluctuations ∼ gravitational potential at $z \sim 1100$ (380000 yr after big bang) ⟹ structure

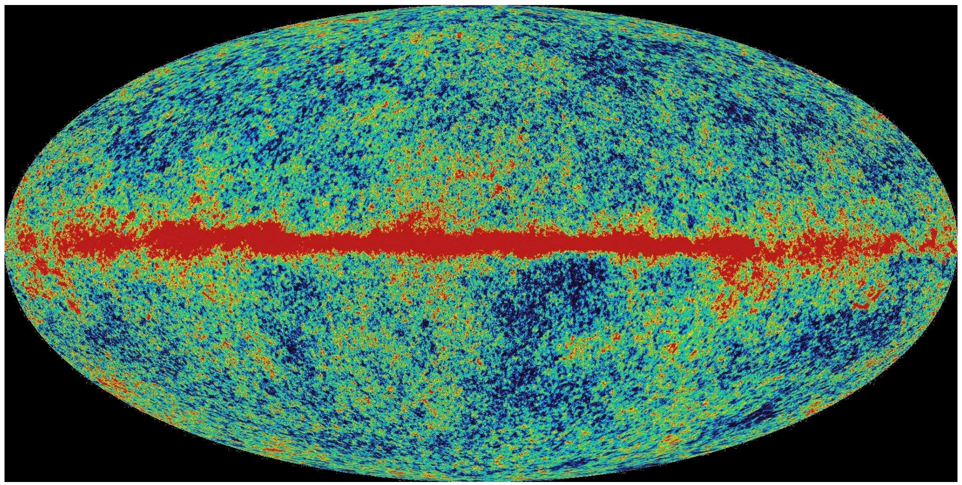

WMAP, W-Band, $\lambda = 3.2\,\mathrm{mm}$, $\nu = 93.5\,\mathrm{GHz}$, resolution 0.21°

The Local Group

Andromeda galaxy (=M31; closest real neighbour galaxy, diam. 20kpc, distance: 675 kpc), NOAO/AURA/NSF

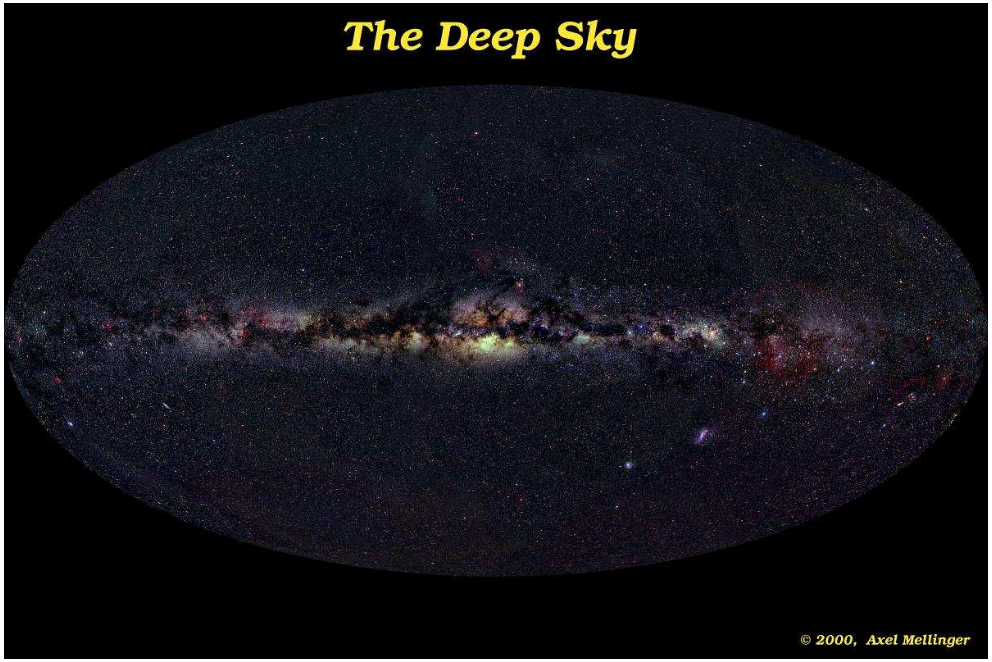

Milky Way

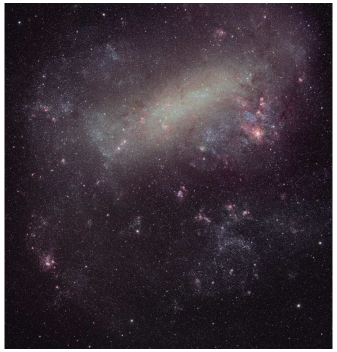

LMC

Loke Kun Tan

Sag Dwarf

HST

Leo Dwarf Galaxy

D. Malin (AAT)

Most other of the $\sim$40 local group galaxies, however, are irregular galaxies, mainly bound to one of the three main members.

M 33 (="Triangulum Galaxy"; $L \sim 0.2 L_{\text{Milky Way}}$)

Table 1: Local Group Galaxies

Galaxy (1)	Other Name (2)	α_{2000} (3)	δ_{2000} (4)	l (5)	b (6)	Type (7)	Subgroup (8)	Images (9)	Notes (10)
WLM	DDO 221	00 01 58	−15 27.8	75.9	−73.6	IrrIV-V	LGC	1	
NGC 55		00 15 08	−39 13.2	332.7	−75.7	IrrIV	LGC	3,4,51	
IC 10	UGC 192	00 20 25	+59 17.5	119.0	−3.3	dIrr	M31	5,6	
NGC 147	DDO 3	00 33 12	+48 30.5	119.8	−14.3	dSph/dE5	M31	7,51	
And III		00 35 17	+36 30.5	119.3	−26.2	dSph	M31	8	
NGC 185	UGC 396	00 38 58	+48 20.2	120.8	−14.5	dSph/dE3p	M31	7,51	
NGC 205	M110	00 40 22	+41 41.4	120.7	−21.1	E5p/dSph-N	M31	7,51	E
M32	NGC 221	00 42 42	+40 51.9	121.2	−22.0	E2	M31	9,10,51	
M31	NGC 224	00 42 44	+41 16.1	121.2	−21.6	SbI-II	M31	10,50,51	
And I		00 45 43	+38 00.4	121.7	−24.9	dSph	M31	8	
SMC	NGC 292	00 52 44	−72 49.7	302.8	−44.3	IrrIV-V	MW	11,12,51	
Sculptor		01 00 09	−33 42.5	287.5	−83.2	dSph	MW	13,49	
LGS 3	Pisces	01 03 53	+21 53.1	126.8	−40.9	dIrr/dSph	M31	14	
IC 1613	DDO 8	01 04 54	+02 08.0	129.8	−60.6	IrrV	M31/LGC	15-17	
And II		01 16 27	+33 25.7	128.9	−29.2	dSph	M31	8	A
M33	NGC 598	01 33 51	+30 39.6	133.6	−31.3	ScII-III	M31	17,18,51	
Phoenix		01 51 06	−44 26.7	272.2	−68.9	dIrr/dSph	MW/LGC	19,20	
Fornax		02 39 59	−34 27.0	237.1	−65.7	dSph	MW	21	
EGB 0427+63	UGCA 92	04 32 01	+63 36.4	144.7	+10.5	dIrr	M31	23	
LMC		05 23 34	−69 45.4	280.5	−32.9	IrrIII-IV	MW	11,12,51	
Carina		06 41 37	−50 58.0	260.1	−22.2	dSph	MW	24	
Leo A	DDO 69	09 59 24	+30 44.7	196.9	+52.4	dIrr	MW/N3109	29,51	
Sextans B	DDO 70	10 00 00	+05 19.7	233.2	+43.8	dIrr	N3109	27,28,51	
NGC 3109	DDO 236	10 03 07	−26 09.5	262.1	+23.1	IrrIV-V	N3109	29,30,51	
Antlia		10 04 04	−27 19.8	263.1	+22.3	dIrr/dSph	N3109	31	B
Leo I	DDO 74	10 08 27	+12 18.5	226.0	+49.1	dSph	MW	32	
Sextans A	DDO 75	10 11 06	−04 42.5	246.2	+39.9	dIrr	N3109	33,51	
Sextans		10 13 03	−01 36.9	243.5	+42.3	dSph	MW	34	
Leo II	DDO 93	11 13 29	+22 09.2	220.2	+67.2	dSph	MW	52	
GR 8	DDO 155	12 58 40	+14 13.0	310.7	+77.0	dIrr	GR8	36,37,54	
Ursa Minor	DDO 199	15 09 11	+67 12.9	105.0	+44.8	dSph	MW	38	
Draco	DDO 208	17 20 19	+57 54.8	86.4	+34.7	dSph	MW	39	
Milky Way		17 45 40	−29 00.5	0.0	0.0	Sbc	MW		
Sagittarius		18 55 03	−30 28.7	5.6	−14.1	dSph-N	MW	40	E
SagDIG	UKS1927-177	19 29 59	−17 40.7	21.1	−16.3	dIrr	LGC	41,53	
NGC 6822	DDO 209	19 44 56	−14 48.1	25.3	−18.4	IrrIV-V	LGC	42,43,51	
DDO 210	Aquarius	20 46 46	−12 51.0	34.0	−31.3	dIrr/dSph	LGC	36,44,54	C
IC 5152		22 02 42	−51 17.7	343.9	−50.2	dIrr	LGC	51	
Tucana		22 41 50	−64 25.2	322.9	−47.4	dSph	LGC	47,48	D
UKS2323-326	UGCA 438	23 26 27	−32 23.3	11.9	−70.9	dIrr	LGC	41	
Pegasus	DDO 216	23 28 34	+14 44.8	94.8	−43.5	dIrr/dSph	LGC	25,44,51	

EXPLANATION OF COLUMNS OF TABLE 1:
Column 1: Galaxy name. Entries denoted in *italics* refer to the five giant Local Group galaxies that are not discussed in this review in any detail; *Columns 2:* A common alternative name; *Columns 3 and 4:* Right ascension and declination for epoch J2000.0, respectively; *Columns 5 and 6:* Galactic longitude and latitude, respectively; *Column 7:* Galaxy type following van den Bergh (1994a); *Column 8:* Subgroup membership within the Local Group; *Column 9:* References to optical and 21-cm images (if available); *Column 10:* Special notes.

NOTES FOR TABLE 1:

A. The position listed here is based on an independent measurement by Paul Hodge (private communication).
B. Also known as PGC 29194 (Fouqué et al 1990) before it was re-discovered as a probable Local Group member by Whiting et al (1997). A thorough discussion of 'pre-discovery' observations of Antlia is provided by Aparicio et al (1997a).
C. Marconi et al (1990) claimed that the original position of DDO 210 (Fisher and Tully 1975) was significantly in error. However, Lo et al (1993) noted that the original position seemed to be correct, and Marconi et al (1995) subsequently agreed. The position listed here corresponds to the original one from Fisher and Tully (1975).
D. Tucana was known prior to its re-discovery by Lavery and Mighell (1992) who thoroughly document all listings of the galaxy in earlier catalogs. Lavery and Mighell (1992) did first claim Tucana to be a possible Local Group member.
E. The 'N' suffix has been added to indicate that these systems may be nucleated dwarfs.

REFERENCES FOR TABLE 1: [1] Sandage & Carlson (1985b); [2] Lautsen et al (1977); [3] Hummel et al (1986); [4] Puche et al (1991); [5] de Vaucouleurs & Ables (1965); [6] Shostak & Skillman (1989); [7] Young & Lo (1997a); [8] Caldwell et al (1992); [9] Kent (1987); [10] Hodge (1981); [11] de Vaucouleurs & Freeman (1972); [12] Mathewson & Ford (1984); [13] Carignan et al (1998); [14] Young & Lo (1997b); [15] Ables (1971); [16] Lake & Skillman (1989); [17] Sandage (1961); [18] Corbelli et al (1989); [19] van de Rydt et al (1991); [20] Carignan et al (1991); [21] Hodge (1971); [22] Saha & Hoessel (1991); [23] Hoessel et al (1988); [24] Smecker-Hane et al (1994); [25] Sandage (1986b); [26] Young & Lo (1996a); [27] Sandage & Carlson (1985a); [28] Skillman et al (1988); [29] Sandage & Carlson (1988); [30] Jobin & Carignan (1990); [31] Whiting et al (1997); [32] Hodge (1963a); [33] Sandage & Carlson (1982); [34] Mateo et al (1995a); [35] Deleted; [36] Fisher & Tully (1979); [37] Carignan et al (1990); [38] van Agt (1967); [39] Baade & Swope (1961); [40] Ibata et al (1997); [41] Longmore et al (1978); [42] Hodge (1978); [43] Gottesman & Weliachew (1977); [44] Lo et al (1993); [45] Deleted; [46] Deleted; [47] Lavery & Mighell (1992); [48] Oosterloo et al (1996); [49] van Agt (1978); [50] Hodge (1992a); [51] Sandage & Bedke (1994); [52] Vogt et al (1995); [53] Cesarsky et al (1977); [54] Hopp & Schulte-Ladbeck (1995).

(Mateo, 1998, Tab. 1)

Our Backyard: The Local Group

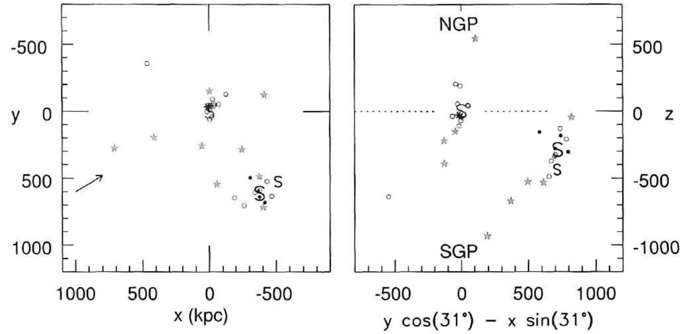

SG, Fig. 4.2; see also `http://www.astro.umass.edu/~fardal/localvol/index.php`

Distribution of galaxies in local group is not random: hierarchy of galaxies:

- small galaxies surround massive ones
- Milky Way satellites lie in plane $\Longrightarrow$ joint formation?
- however, many small galaxies are *not* associated with large galaxies

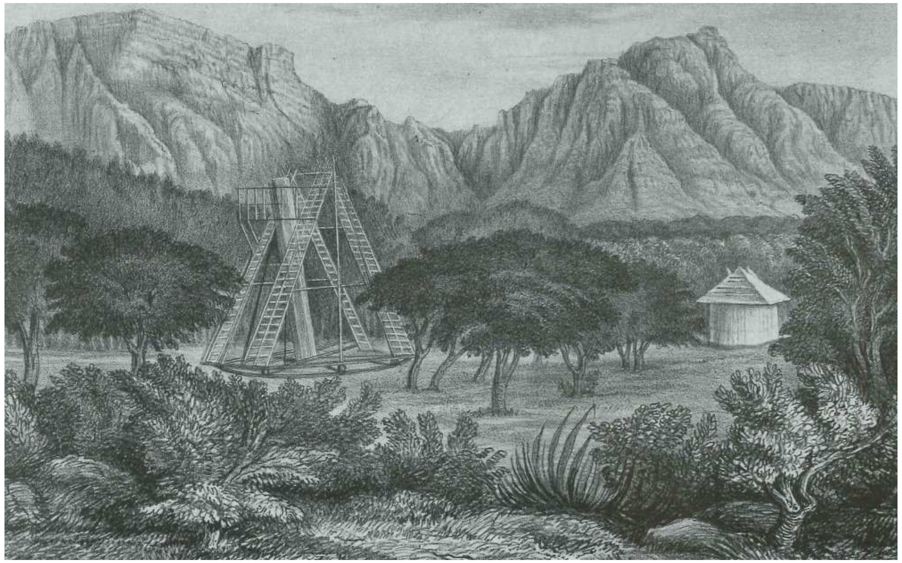

Block & Freedman, 2008, Fig. 40

21 Foot telescope of John Herschel in Feldhausen (table mountain, close to cape town; 1825–1838)

J. Herschel (1851): *. . . there are nebulae in abundance both regular and irregular, globular clusters in every state of condensation, and objects of a nebulous character quite peculiar, which have no analogue in any other region of the heavens. . .*

Our Backyard: The Local Group

Types of Galaxies:

- two spirals, but only one large elliptical
- rich in 'late type galaxies', i.e., spirals and irregulars
- poor in 'early type' giant ellipticals and S0 galaxies

$\Longrightarrow$ Typical for groups (not(!) for galaxy clusters!)

Dynamics:

- Andromeda and Galaxy are approaching at $\sim$120 km s^{-1}
- All other galaxies within of 60 km s^{-1} of Andromeda/Milky Way

$\Longrightarrow$ Local Group is gravitationally bound

Half of all (known) galaxies are in groups or clusters, other half in loose associations.

$\Longrightarrow$ Local group is hopefully a typical groups, so will study this here.

Big advantage: these are the last galaxies we can resolve into stars.

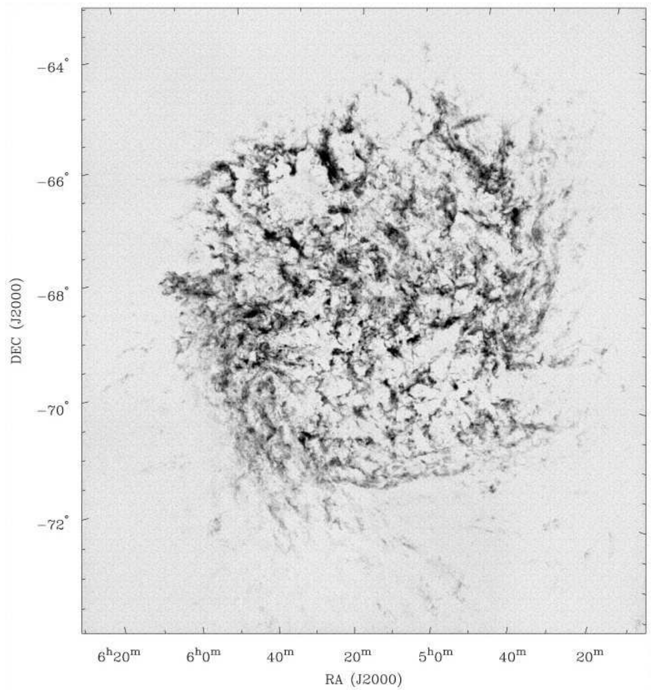

(Kim et al., 1998, Fig. 1)

Large Magellanic Cloud:

- distance: 49 kpc
- Size 15° × 13° ($\sim$14 kpc)
- Prototype of Magellanic Spirals (Sm)
- Morphology: from 21 cm: flat disk, tilted by $\sim$45° against plane of sky

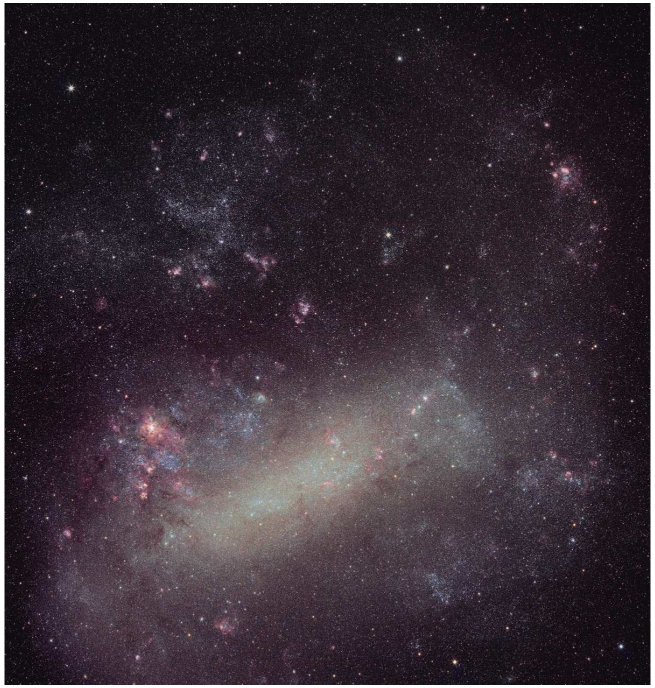

Optical: “cigar structure” of stars, many star formation regions visible through Hα emission.

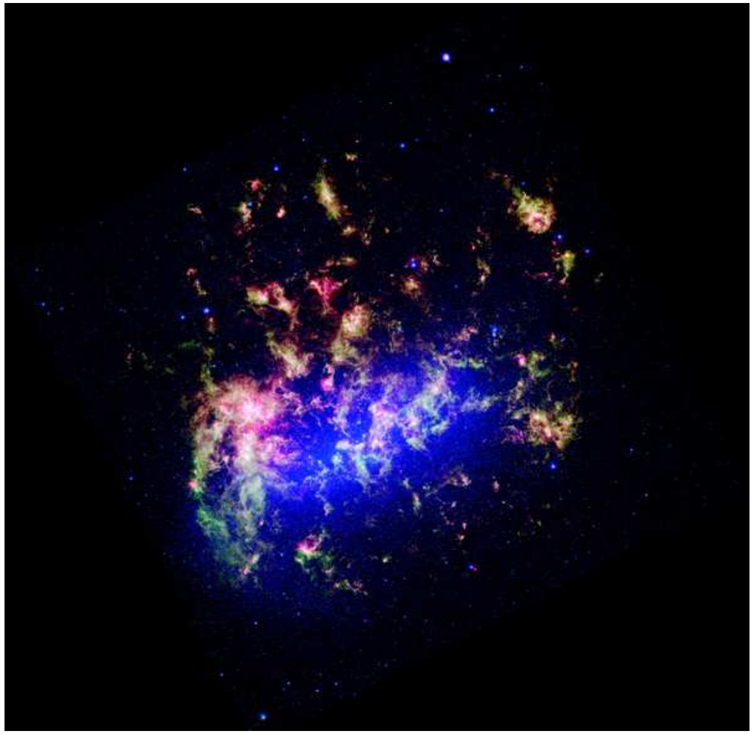

SAGE (Meixner et al., 2006): Infrared mapping of the LMC with Spitzer: blue: IRAC-1 3.6 μm, green: IRAC-4 8 μm, red: MIPS

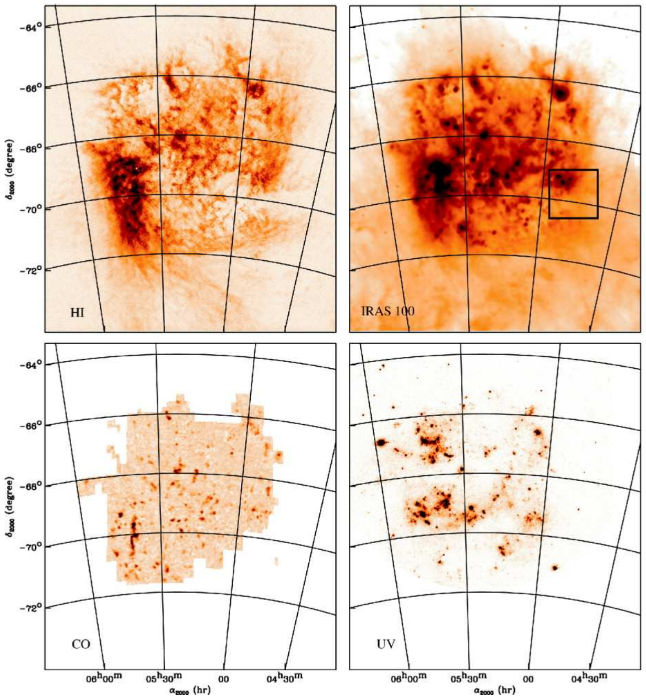

Distribution of emission in different bands:

- H I: cold gas
- IRAS: warm gas/dust
- CO: molecular clouds (star formation!)
- UV: hot stars (star formation!)

Note holes and loops: SNe and hot stars push colder ISM aside $\Longrightarrow$ hot bubbles

Such structure is typical for irregular galaxies

1987 February: Supernova in Large Magellanic Cloud.

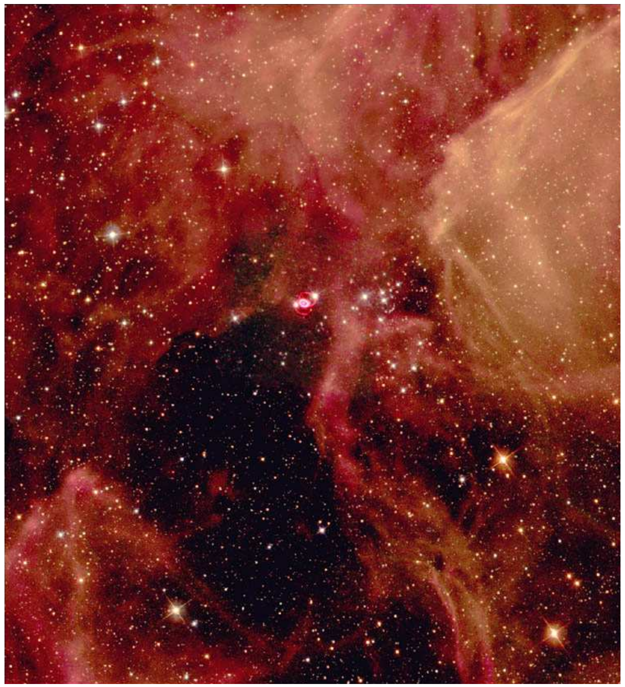

HST/NASA/ESA/STScI

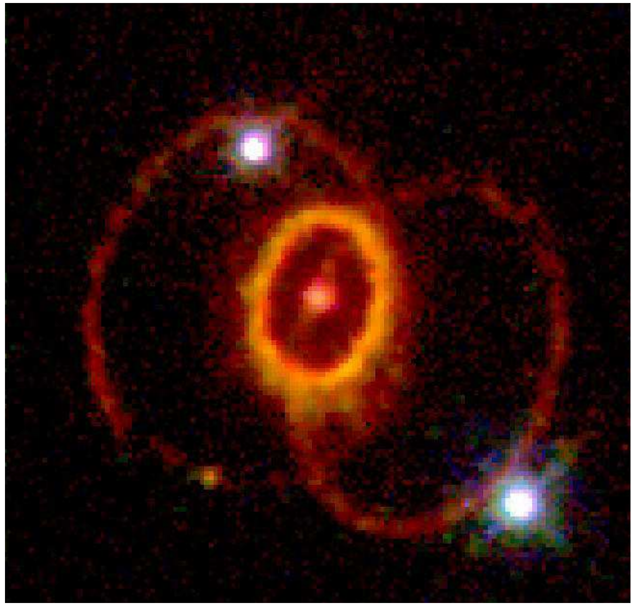

STScI PR94-22

87 d after explosion: Ring ($1.66'' \times 1.21''$) of ionized C and N around SN

$\Longrightarrow$ Excitation of C, N in ring-like shell (ejecta from red giant phase of progenitor?): "light echo"

LMC: Distance, V

Light echo: direct geometrical determination of distance to LMC possible:

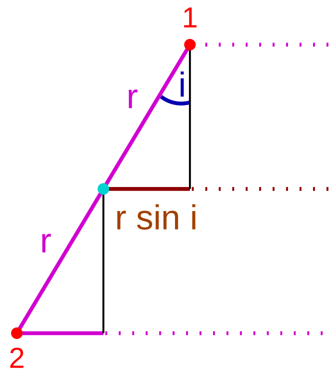

Time delay SN: close side of ring:

$$ct_1 = r(1 - \sin i) = 86 \pm 6\,\mathrm{d} \quad (3.1)$$

Time delay SN: far side of ring:

$$ct_2 = r(1 + \sin i) = 413 \pm 24\,\mathrm{d} \quad (3.2)$$

The ring radius is:

$$r = c\,\frac{t_1 + t_2}{2} = 250 \pm 12\,\mathrm{ltd} \quad (3.3)$$

and the inclination is:

$$\sin i = \frac{t_2 - t_1}{t_1 + t_2} \Longrightarrow i \sim 41^\circ \quad (3.4)$$

(From ring-geometry: $\cos i = 1''.21/1''.66 \Longrightarrow i \sim 43^\circ$)

Thus from angular size of ring:

$$1''.66 = \frac{r \cos i}{d} \Longrightarrow d = 52 \pm 3\,\mathrm{kpc} \quad (3.5)$$

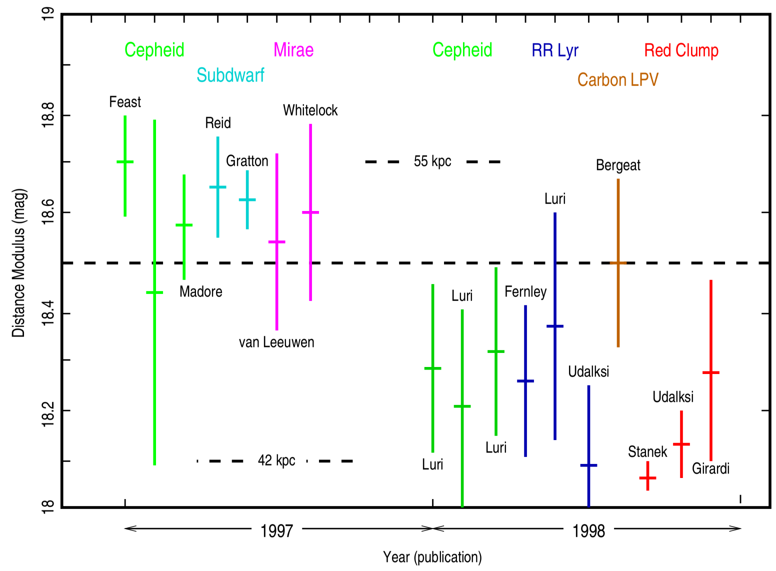

LMC distance: "anchor point" of extragalactic distance scale.

After Gaia Science Workgroup

Strong dependence on Hipparcos calibration.

DM ranges between 18.7 ± 0.1 mag (Feast & Catchpole) and 18.57 ± 0.11 mag (Madore & Freedman)

Currently, the distance to the LMC is less well known than desirable.

LMC: Metallicity

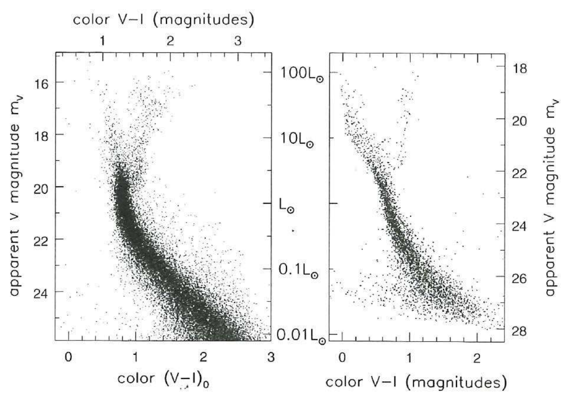

Sparke & Gallagher, Fig. 4.5

CMD of bulge stars in the MW — CMD of stars in LMC

Wide main sequence ⟹ dispersion in stellar ages

LMC: MS is bluer ⟹ LMC has lower metallicity

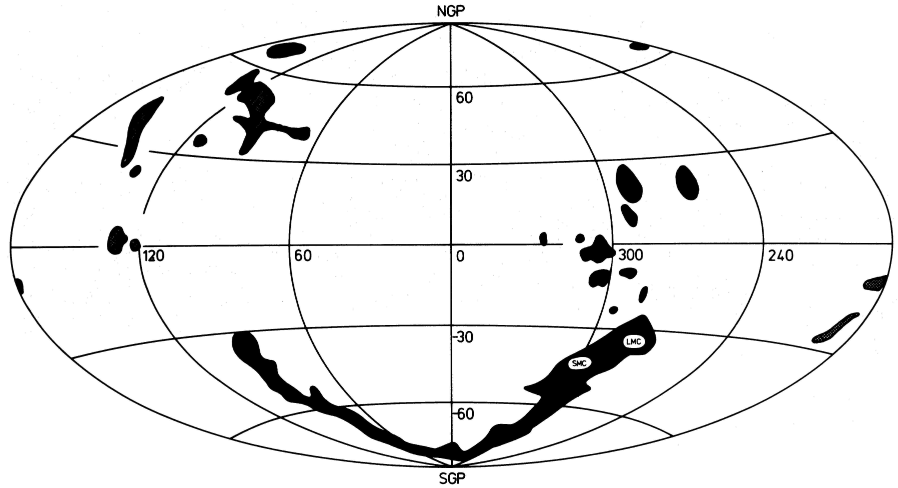

Mathewson et al. (1974, Fig. 1):

Magellanic Stream: number of high velocity clouds trailing Magellanic clouds

Total mass: $2 \times 10^8 M_\odot$.

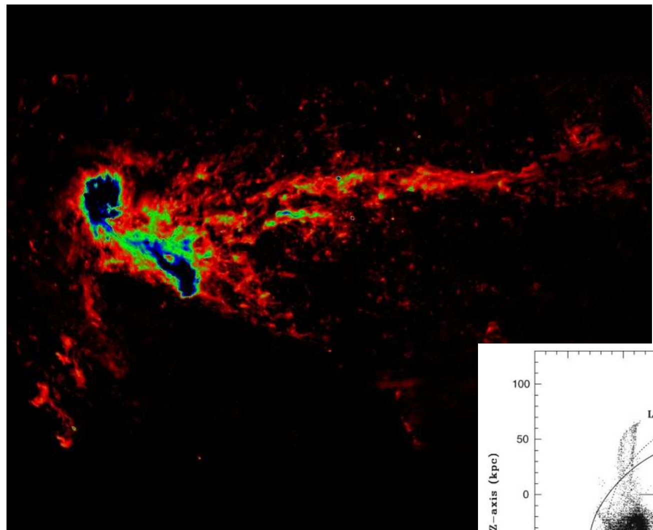

(Putman et al., 2003)

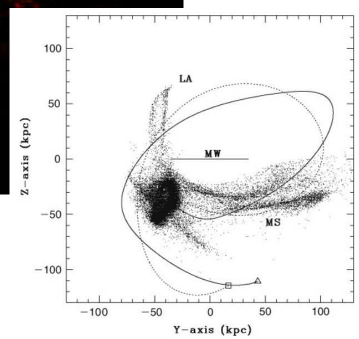

HIPASS-Survey (Putman et al., 2003): 21 cm survey spanning whole southern sky.

first real map of Magellanic Stream.

Head of stream: gas freshly removed from LMC and SMC,

tail: older material

(Bekki & Chiba, 2009, Fig. 3)

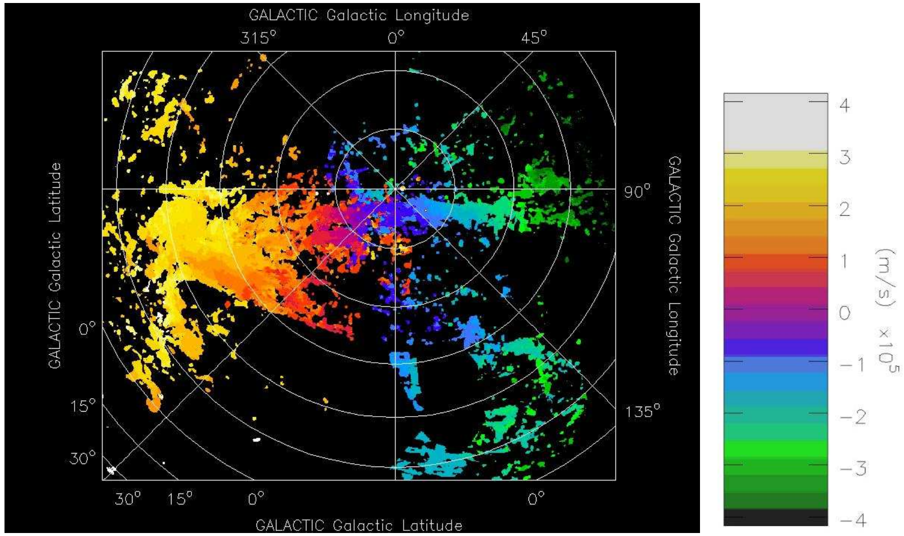

(Putman et al., 2003)

Velocity field from HIPASS-Survey

Stream has gradient of $\sim$700 km s^{-1}, $\sim$390 km s^{-1} faster than galactic rotation

$\Longrightarrow$ noncircular orbit

R. Gendler

General Properties, II

Andromeda galaxy:

- diameter 20 kpc, distance 675 kpc
- $\sim$50% more luminous than Galaxy
- faster rotation speed ($\sim$260 km/s)
- 300 globular clusters
- many satellites:
  - one elliptical galaxy (M32)
  - three dwarf ellipticals
  - at least six dwarf spheroidals

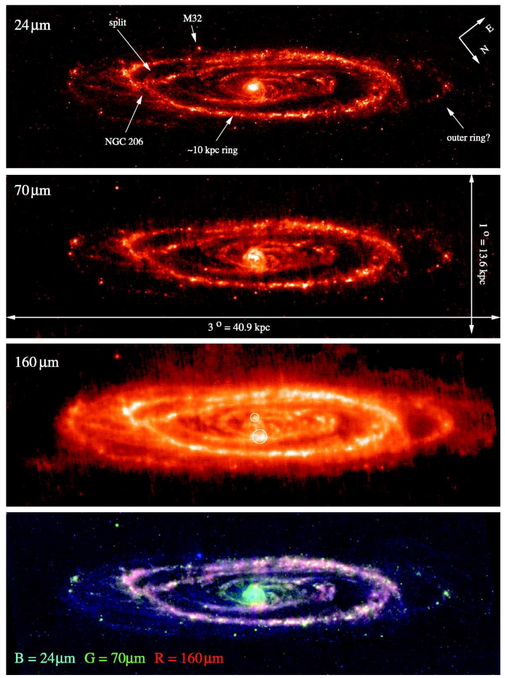

Dust distribution in M31:

- "ring of fire" at $\sim$10 kpc
- contains most young stars
- also contains ionized H II regions (see last lecture)

(Gordon et al., 2006, Fig. 1)

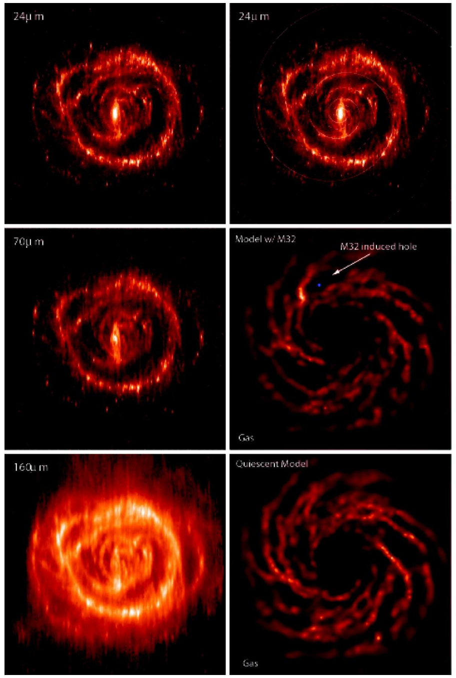

Deprojected images of Andromeda assuming inclination of 75°

Note clear spiral structure, but disturbed by passage of M32 (first seen by ISO).

Movie time: `gordon_video1.mpg`

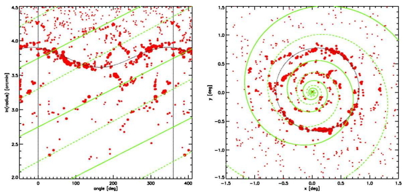

Ring is off-center, not associated directly with spiral arms (modeled by logarithmic spiral); origin not completely clear.

(Gordon et al., 2006, Figs. 3 and 4)

Dust

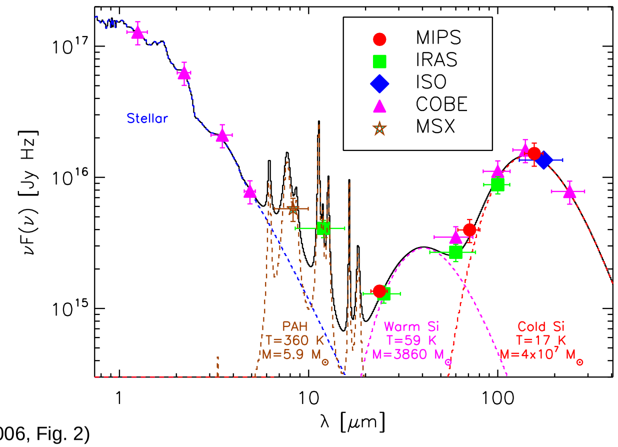

(Gordon et al., 2006, Fig. 2)

Total IR luminosity: $1.7 \times 10^{43}\,\mathrm{erg\,s^{-1}}$, corresponding to star formation rate of $0.75\,M_\odot\,\mathrm{yr}^{-1}$.

Dust composition: silicates (warm from inner regions, cold from outer regions of Galaxy) and some polycyclic aromatic hydrocarbons (PAHs)

Milky Way and M31

M31 and Milky Way are gravitationally bound and approaching on a collision course, with collision happening in 2 billion years.

Possible scenario: formation of an elliptical galaxy over the course of about 1 billion years.

Collision studied with numerical simulations, movies show evolution calculations using 307.2 million particles (10 days on 512 processors):

MOVIE Time: `hdmwa.mov` and `7_FutureSky.avi` from `http://www.cita.utoronto.ca/~dubinski/nbody/`

M51, NOAO, T. Rector

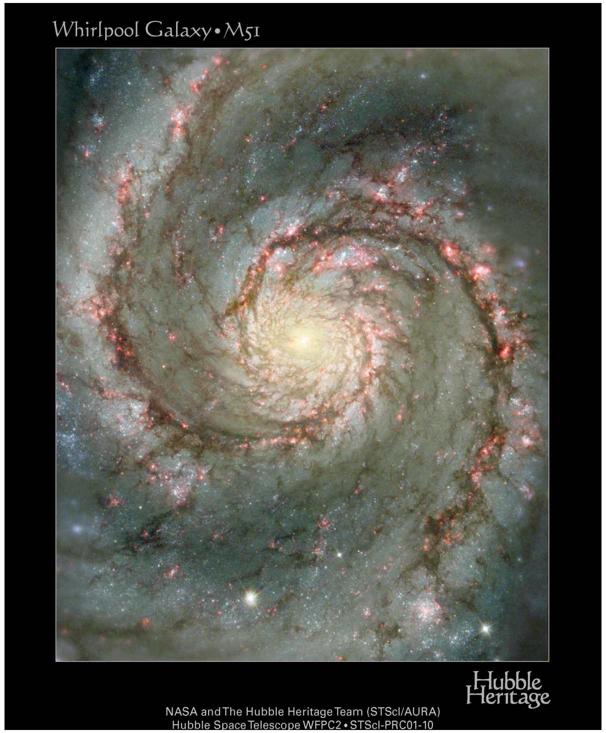

NGC 4565, McLaughlin

Star Forming Region RCW 108 in ARA
(MPG/ESO 2.2-m + WFI)

ESO PR Photo 21a/99 (30 April 1999)

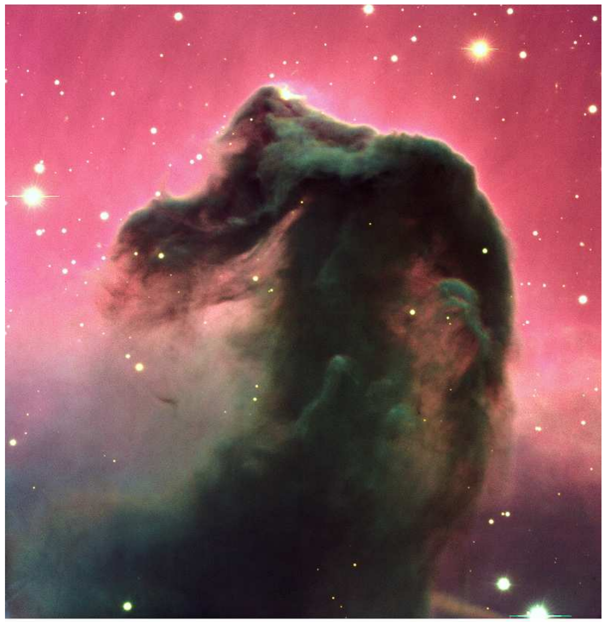

The Horsehead Nebula
(VLT KUEYEN + FORS 2)

ESO PR Photo 02a/02 (25 January 2002)

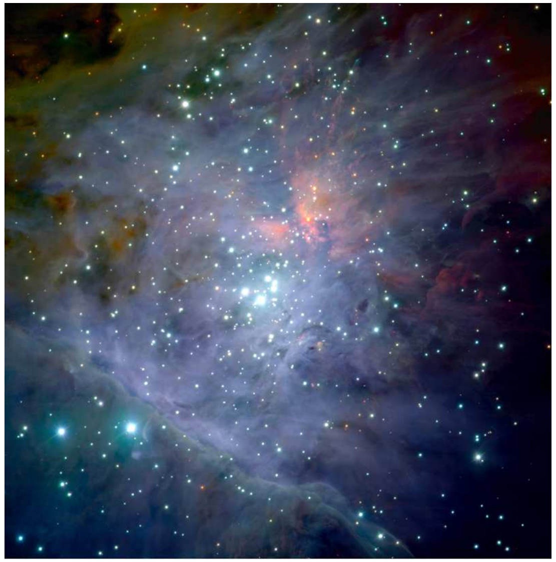

The Orion Nebula and Trapezium Cluster
(VLT ANTU + ISAAC)

ESO PR Photo 03a/01 (15 January 2001) © European Southern Observatory

Milky Way: ISM

The ISM of the Milky Way consists of the following phases

Name	Type	n cm^{-3}	T K	Filling Factor Vol-%	Mass % ISM	Comments
HIM	H II	10^{-2}–10^{-4}	10^6–10^8	20–60	<1	SNR, wind, shocks
WIM	H II	10^{-1}–10^{-4}	10^4	1–10	<1	photoionized by O/B-stars
WNM	H I	1–10	10^4	20–30	20-50	21cm clouds, shells
CNM	H I	10–10^2	100	10–20	20-50	HI envelopes, shells
MC	H I	10^2–10^4	10	1	40-50	IR, dust

HIM: Hot Ionized Medium, WIM: Warm Ionized Medium, WNM: Warm Neutral Medium, CNM: Cool Neutral Medium, MC: Molecular Clouds

courtesy J. Bally

Molecules: History

- Secchi, 1878: First notice of molecular features in stellar spectra (class III and IV; no explanation)
  Today known as TiO, C_2, and CN bands
- 1930s: Molecular lines in spectra of planetary atmospheres and comets as well as low temperature stars
- 1941: Interstellar absorption lines due to CN, CH, and CH^+ in optical spectrum of ζ Oph
- Weinreb et al, 1963: Radio absorption lines at $\lambda = 18\,\mathrm{cm}$ from OH towards SNR Cas A (not associated with Cas A, but with foreground clouds). masers (=non-LTE!)
- Cheung et al., 1968: First multi-atom molecules: NH_3 and H_2O ($\lambda = 1.35\,\mathrm{cm}$).
- Snyder et al., 1969: Formaldehyde (H_2CO).
- Today: more than 120 different molecules known

Molecular Hydrogen, I

Because of high abundances: most molecular gas is H_2.

For review of properties of H_2, see Shull & Beckwith, 1982, Ann. Rev. Astron. Astrophys. 20, 163

H_2 is homonuclear

$\Longrightarrow$ no permanent dipole moment

$\Longrightarrow$ no rotational dipole transitions.

Only transitions observable are vibrational or electronic.

Vibrational: $\lambda \sim 6\,\mu$m, in the infrared.

Problem: Dust extinction in IR severe

Once H is molecular, it is very difficult to see.

Alternative: Observation of electronic transitions of H_2 in absorption against hot UV-Stars ("Werner-bands").

Note that excitation of transitions requires lots of energy which cannot be produced otherwise.

Molecular Hydrogen, II

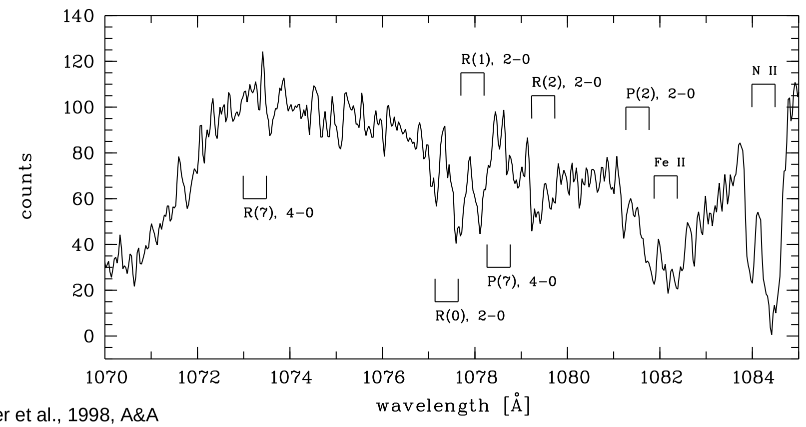

Richter et al., 1998, A&A

ORFEUS: Discovery of H_2 bands in absorption in direction towards SMC

$\Longrightarrow$ H_2 also present in diffuse ISM, not only in clouds

(agrees with *Copernicus* measurements in milky way; Spitzer, 1974)

Molecular Hydrogen, III

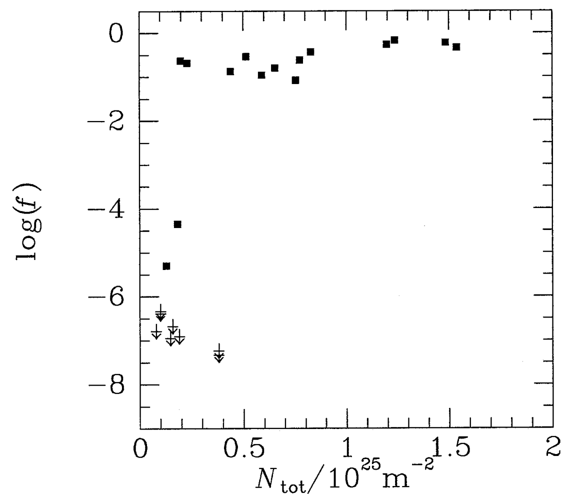

Binney&Merrifield, Fig. 8.5

Calculate total Hydrogen-density obtained from

$$N(\mathrm{H_{tot}}) = N(\mathrm{HI}) + 2N(\mathrm{H_2}) \quad (3.6)$$

and molecular fraction

$$f_{\mathrm{H_2}} = \frac{2N(\mathrm{H_2})}{N(\mathrm{H_{tot}})} \quad (3.7)$$

For $N(\mathrm{H_{tot}}) < 2 \times 10^{18}\,\mathrm{cm^{-2}}$, i.e., low columns, H is atomic, above that molecular $\Longrightarrow$ More molecules in denser parts of ISM.

Carbon Monoxide

Better than observing H_2 directly is to deduce its presence *indirectly* using other molecules with rotational positions $\Longrightarrow$ use heteronuclear molecules, e.g., CO, CS, HCN.

Candidate Number 1: CO, rotational transitions at 1.3 mm ($J = 2 \rightarrow J = 1$) and 2.6 mm ($J = 1 \rightarrow J = 0$).

Notation: CO(2-1) and CO(1-0)

CO is less abundant than H_2 (see later), but Einstein A-coefficients of lines very large; $\tau = 1$ reached at CO-column $\sim 6 \times 10^{15}\,\mathrm{cm^{-2}}$, corresponding to $N_\mathrm{H} \sim 8 \times 10^{19}\,\mathrm{cm^{-2}}$

$\Longrightarrow$ Cannot use "standard" CO to look into thick clouds.

$\Longrightarrow$ Use some tricks: Isotope effects!

CO: Isotope Effects

CO occurs in several forms:

- $^{12}C^{16}O$ (= ^{12}CO)
- $^{13}C^{16}O$ (= ^{13}CO)
- $^{12}C^{18}O$ (= $C^{18}O$)

because of slightly different reduced masses, wavelength of transitions slightly different $\Longrightarrow$ can separate emission lines from these species.

Relative abundances:
^{12}CO : ^{13}CO : $C^{18}O$ = 500 : 65 : 1

By using ^{13}CO or $C^{18}O$, can look deeper in molecular cloud.

courtesy Matthew T. Russell

Column from Lines

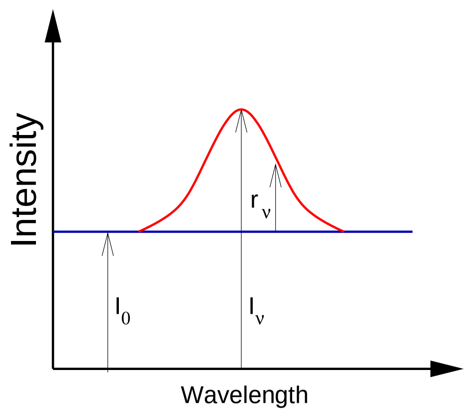

after Cowley, Fig. 14.5

To measure mass from emission line, determine number of emitting atoms, N.

Observed intensity not trivially $\propto N$ because of self-absorption.

Excess in line:

$$r_\nu = \frac{I_\nu - I_0}{I_0} = \frac{S_\nu - I_0}{S_\nu}\left(1 - \exp\left(-\frac{\tau_\nu}{\mu}\right)\right) \quad (3.8)$$

where τ: optical depth, I_0: background intens., $\mu = \cos\theta$

Inserting τ in terms of transition probability f_{nm} and expanding the exponential gives for the equivalent width

$$W_\nu = \int r_\nu \, d\nu \sim \frac{\pi e^2}{mc} r_0 f_{nm} \frac{N_n}{\mu} \quad (3.9)$$

where $r_0 = (S_\nu - I_0)/S_\nu$.

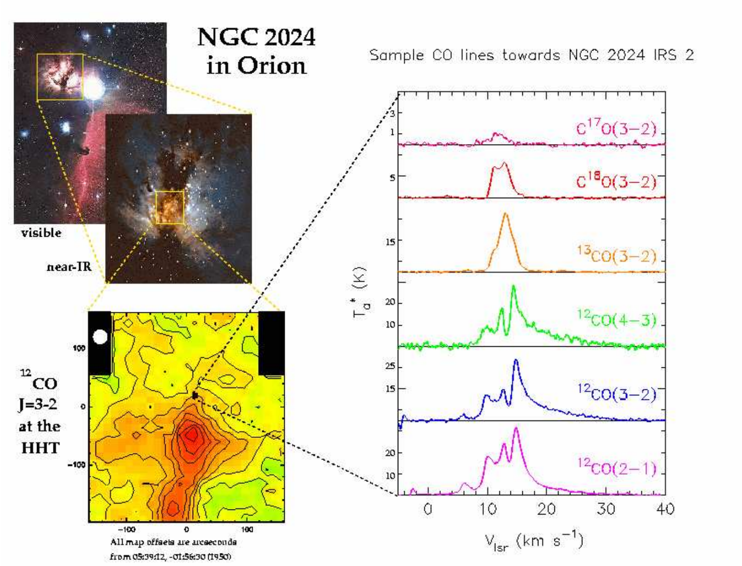

(courtesy Craig Kulesa)

As a case study: use NGC 2024 (flame nebula, bright star is Alnitak [ζ Ori]).

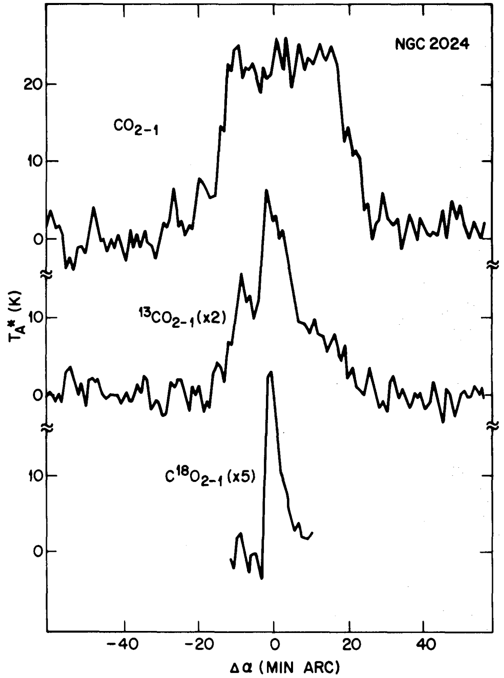

Right-ascension strip maps over NGC 2024: peak intensities ^{12}CO, ^{13}CO, and C^{18}O scale as 5:2:1 $\Longrightarrow$ cloud is optically thick (lines should scale as the abundances, and they don't).

Last step to obtain N_{CO}: use Boltzmann if (and only if) LTE is appropriate...

(Phillips et al., 1979, Fig. 3b), Intensity given as antenna temperature, $I = 2kT\nu^2/c^2$.

From CO to H

Once $N(\text{CO})$ has been determined: Infer H$_2$ column using some "standard" ratio. Typical assumptions:

$$\frac{N(^{13}\text{CO})}{N(\text{H}_2)} \sim 0.5\ldots2.0\times10^{-6} \qquad (3.10)$$

Ratio determined from UV-data on hydrogen and CO measurements at cloud edges (low τ).

Caveats:

- CO usually *not* in LTE for higher J
- $n(\text{H}_2)/n(^{12}\text{C})$, $n(^{12}\text{C})/n(^{13}\text{C})$ affected by astration (passage of ISM through stars), $\Longrightarrow$ $n(^{12}\text{C})/n(^{13}\text{C}) = 20$ at GC, 90 at large Galactic radii,
- Clumpy clouds? Shadowing? (finite beamsize of telescope...),
- Isotope ratios very different between different cloud complexes
- ...

H$_2$ mass only determinable to factor of a few!

Molecular Clouds, I

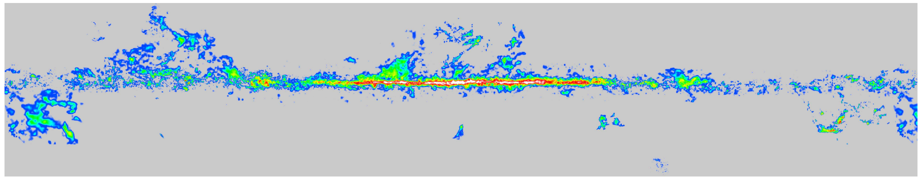

Dame et al., CfA; Columbia 1.2 m telescope

CO distribution in galactic coordinates: concentration of clouds on plane; high speed at center not yet understood.

Molecular Clouds, II

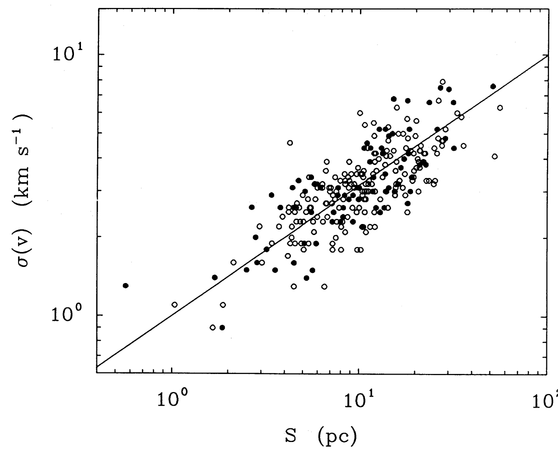

Solomon et al. (1987): 2.6 mm ^{12}CO survey of $>$ 200 molecular clouds within solar circle.

Relationship between velocity dispersion, σ_v, (from line width) and cloud size, S:

$$\sigma_v = (1\pm0.1)\,\text{km}\,\text{s}^{-1}\left(\frac{S}{\text{pc}}\right) \qquad (3.11)$$

(Solomon et al., 1987, Fig. 1)

Molecular Clouds, III

Median linewidth in Solomon survey:

$$\sigma_v \sim 3\,\mathrm{km\,s^{-1}} \tag{3.12}$$

Compare to sound-speed, assuming $kT \sim 30\,\mathrm{K}$

$$c_\mathrm{s} \sim \sqrt{\frac{kT}{m_\mathrm{p}}} \sim 0.5\,\mathrm{km\,s^{-1}}\sqrt{\frac{T}{30\,\mathrm{K}}} \tag{3.13}$$

σ_v dominated by turbulent velocity within clouds, not by sound speed...

Turbulent pressure $P \sim nm\sigma_v^2$, with $n \gtrsim 10^2\,\mathrm{cm^{-3}}$, much higher than confining pressure in intra-cloud medium (there: $n \sim 1\,\mathrm{cm^{-3}}$, $c_s \sim 10\,\mathrm{km\,s^{-1}}$) $\Longrightarrow$ clouds confined by gravity!

Use virial theorem to obtain mass:

$$M \sim \mathrm{const.}\frac{\sigma_v^2 S}{G} \tag{3.14}$$

where const. $\sim$ 8.7, depending on geometry.

Molecular Clouds, IV

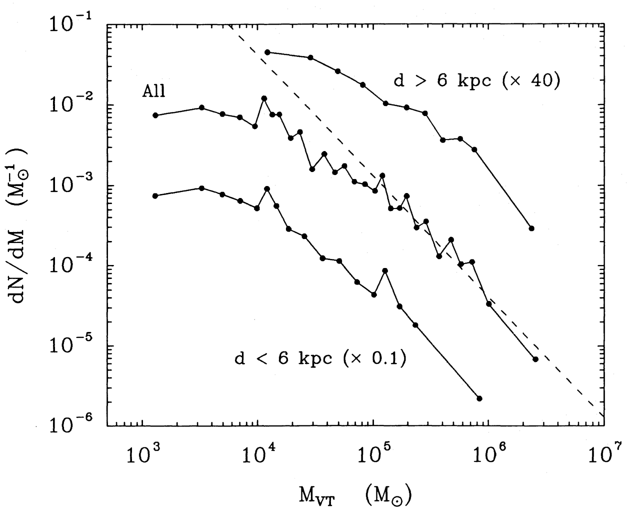

Mass spectrum of molecular clouds is roughly

$$\frac{\mathrm{d}N}{\mathrm{d}M} \propto M^{-1.7} \tag{3.15}$$

for 2000 M$_\odot$ $< M <$ 40000 M$_\odot$.

At low masses selection effect (biasing).

Integrating over mass distribution shows

Most of the Galaxy's molecular gas is in the most massive clouds

(Solomon & Rivolo, 1989, Fig. 1)

Molecule Formation, I

Formation of molecules in dense media (e.g., Earth's atmosphere) is no problem. This is very different from the rest of the universe!

Assume two-body collision of two (neutral) atoms: typical interaction timescale 10^{-13} s (1 vibration timescale).

To form molecule, need to get rid of excess energy!

Problem: Typical time for radiative relaxation given by A-coefficient ($\sim 10^8\,\mathrm{s^{-1}}$)

$\Longrightarrow$ Typical collisional time-scale too low

$\Longrightarrow$ cannot form molecules!

On Earth, excess energy carried away by triple-collisions, these are too rare in the ISM...

Further complication: UV-dissociation of molecules.

Molecule Formation, II

Solution: "nonstandard chemistry", i.e., Atom-ion reactions and dust as catalyst

Atom-ion reactions are, e.g.,

$$\mathrm{O^+ + H_2 \rightarrow OH^+ + H} \tag{3.16}$$

These reactions are very effective since the ion polarizes the molecule.

Langevin theory:

Assume charge q_1 approaches molecule; represent induced dipole-moment by charge q_2 separated by distance p. Then

$$q_2 p = \alpha E \tag{3.17}$$

where E electric field, α polarizability. Since $E = q_1/r^2$, this means

$$p = \frac{\alpha q_1}{q_2 r^2} \tag{3.18}$$

and the attractive force is

$$F_r = -\frac{2q_1q_2p}{r^3} = -\frac{2q_1^2\alpha}{r^5} \tag{3.19}$$

Molecule Formation, III

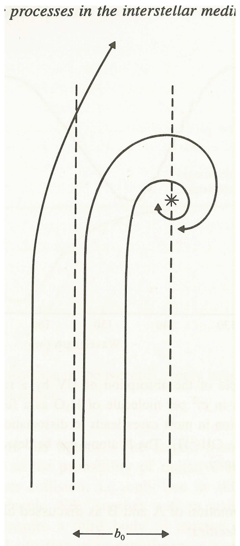

Thus the potential energy is

$$V(r) = \int_r^\infty F_r \, \mathrm{d}r = \frac{q_1^2 \alpha}{2r^4} \tag{3.20}$$

Motion in such a potential allows spiral-in (F can not always be balanced by centrifugal force).
This happens for impact parameters $b < b_0$ where

$$b_0 = q_1 \left(\frac{4\alpha}{\mu v^2}\right)^{1/4} \tag{3.21}$$

where μ is the reduced mass.
$\Longrightarrow$ Langevin cross section

$$Q = \pi b_0^2 \propto \frac{1}{v_\infty} \tag{3.22}$$

Since the collision frequency $\propto \langle Qv \rangle$, collision frequency is independent of energy

Not really true in full theory, but dependence small for regime of astrophysical interest.

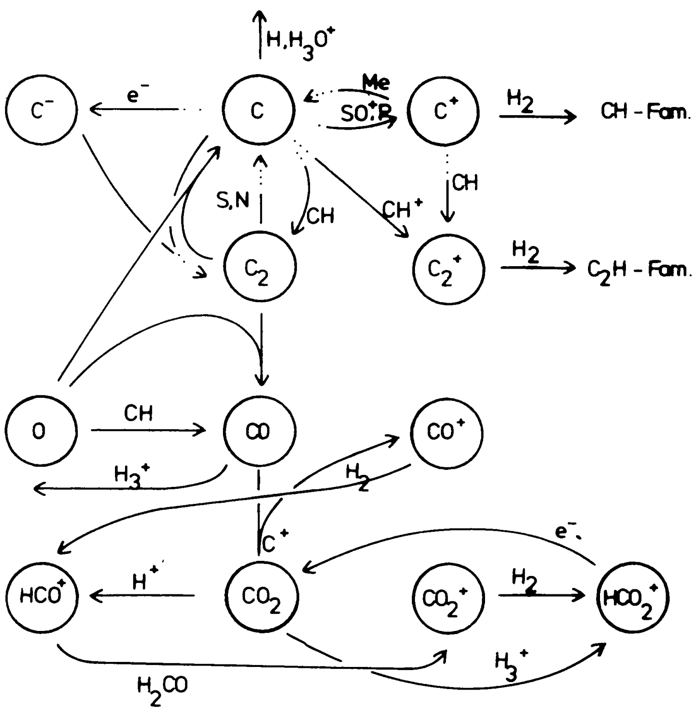

Typical theory of molecular formation: reaction networks with ~1000 and more different reactions.

Henning, 1981

Hydrogen Molecule

One unavoidable fact: we cannot produce H_2 in gas phase $\Longrightarrow$ this must occur on surface of dust grains.

Why?

Two-body recombination is not possible because H_2 has no dipole moment $\Longrightarrow$ radiative relaxation would go via quadrupole terms, which is very slow.

Therefore: the general picture is:

adsorption of H on grain surface (e.g., ice, silicate) $\Longrightarrow$ proton will thermally “hop” over surface (tunnel through lattice structure,...) $\Longrightarrow$ Two H-atoms meet $\Longrightarrow$ formation of H_2

Detailed theory requires knowledge about grains.

Dust

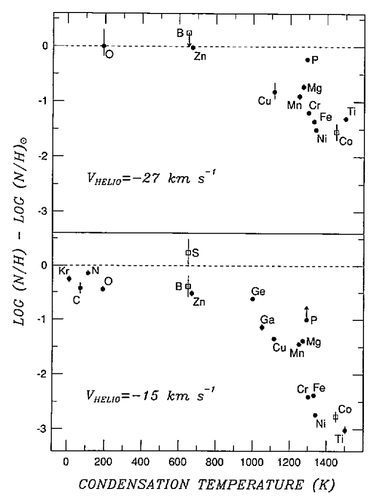

Evidence for existence of solid state material in universe comes mainly from two observations:

1. Depletion of elements in ISM gas phase wrt. solar abundances
2. Reddening of stars

Abundances in direction to ζ Oph (Federman et al., 1993)

3–58

Extinction, I

Extinction = dimming of starlight by dust

How is this measured?

Assume two stars, 1,2, at distances d_1, d_2, with same physical spectral shape, $F(\lambda)$. Medium to star 2 has optical depth $\tau(\lambda)$. Observed spectral fluxes are

$$F_1(\lambda) = \frac{F(\lambda)}{d_1^2} \quad \text{and} \quad F_2(\lambda) = \frac{F(\lambda)}{d_2^2}\mathrm{e}^{-\tau(\lambda)} \tag{3.23}$$

Compare fluxes at wavelength λ_1:

$$\frac{F_1(\lambda_1)}{F_2(\lambda_1)} = \frac{F(\lambda_1)/d_1^2}{F(\lambda_2)/d_2^2}\mathrm{e}^{\tau(\lambda_1)} = \frac{d_2^2}{d_1^2}\mathrm{e}^{\tau(\lambda_1)} \tag{3.24}$$

Same at λ_2:

$$\frac{F_1(\lambda_2)}{F_2(\lambda_2)} = \frac{d_2^2}{d_1^2}\mathrm{e}^{\tau(\lambda_2)} \tag{3.25}$$

Therefore

$$\frac{F_1(\lambda_1)/F_1(\lambda_2)}{F_2(\lambda_1)/F_2(\lambda_2)} = \mathrm{e}^{\tau(\lambda_1)-\tau(\lambda_2)} \tag{3.26}$$

3–59

Extinction, II

Take the logarithm of both sides and multiply with -2.5:

$$-2.5\log\left(\frac{F_1(\lambda_1)}{F_1(\lambda_2)}\right) - \left(-2.5\log\left(\frac{F_2(\lambda_1)}{F_2(\lambda_2)}\right)\right) = \text{const.}\cdot(\tau(\lambda_1)-\tau(\lambda_2)) \tag{3.27}$$

Now remember the definition of the magnitude

$$m(\lambda_1) - m(\lambda_2) = -2.5\log\frac{F(\lambda_1)}{F(\lambda_2)} \tag{3.28}$$

Therefore Eq. (3.27) reads

$$(m_1(\lambda_1)-m_1(\lambda_2)) - (m_2(\lambda_1)-m_2(\lambda_2)) = \text{const.}\cdot(\tau_1-\tau_2) \tag{3.29}$$

In astronomy, a color is defined as a difference of magnitudes, e.g. for the B- and V-filters:

$$\mathrm{B}-\mathrm{V} = m(\mathrm{B}) - m(\mathrm{V}) \tag{3.30}$$

Thus, Eq. (3.29) is difference between colors, or color excess

$$E_{\lambda_1-\lambda_2} := (m_1(\lambda_1)-m_1(\lambda_2)) - (m_2(\lambda_1)-m_2(\lambda_2)) \tag{3.31}$$

Note that because of Eq. (3.29)

$$E_{\lambda_1-\lambda_2} \propto \tau_1 - \tau_2 \tag{3.32}$$

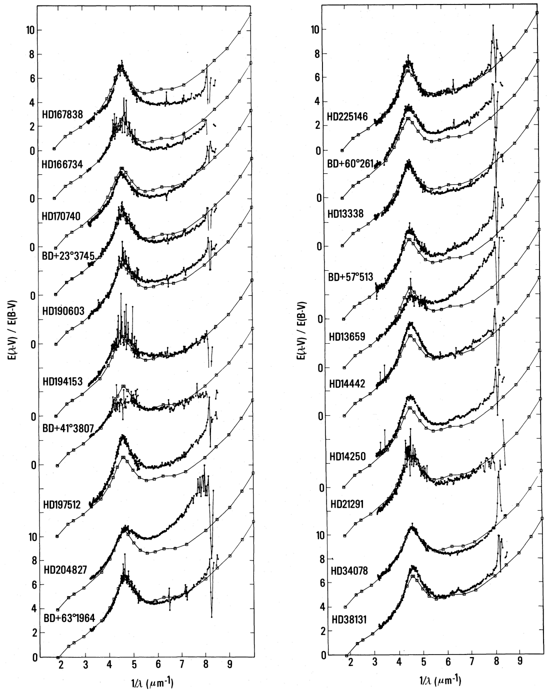

Generally, we use normalized color excess,

$$\frac{E(\lambda-\mathrm{V})}{E(\mathrm{B}-\mathrm{V})} = \frac{\tau(\lambda)-\tau(\mathrm{V})}{\tau\mathrm{B}-\tau\mathrm{V}} \tag{3.33}$$
$$\propto \frac{\tau(\lambda)-\tau(\mathrm{V})}{\tau(\mathrm{B})-\tau(\mathrm{V})} \tag{3.34}$$
$$\propto \tau(\lambda) \tag{3.35}$$
$$\propto \sigma_{\mathrm{sca}}(\lambda) \tag{3.36}$$

Stellar spectra in the UV (Witt et al., 1984): Overall the extinction is very similar, there is a prominent feature at $1/\lambda \sim 4.6$ ($\lambda = 2170$ Å), the strength of the feature varies, but its position is very stable.

3–61

Extinction, IV

Observationally important is relationship between reddening $E(\mathrm{B}-\mathrm{V})$ and extinction in V-band.

Extinction defined via

$$A_\mathrm{V} = \mathrm{V} - \mathrm{V}_0 \tag{3.37}$$

Now, normalized extinction was

$$\frac{E(\lambda-\mathrm{V})}{E(\mathrm{B}-\mathrm{V})} = \frac{(m_\lambda - m_\mathrm{V}) - (m_\lambda - m_\mathrm{V})_0}{E(\mathrm{B}-\mathrm{V})} \tag{3.38}$$
$$= \frac{m_\lambda - m_{\lambda,0} - (m_\mathrm{V} - m_{\mathrm{V},0})}{E(\mathrm{B}-\mathrm{V})} \tag{3.39}$$
$$= \frac{A_\lambda - A_\mathrm{V}}{E(\mathrm{B}-\mathrm{V})} \tag{3.40}$$

But for $\lambda \to \infty$:

$$\frac{E(\lambda-\mathrm{V})}{E(\mathrm{B}-\mathrm{V})} \to \text{const.} =: R \tag{3.41}$$

where $R \sim 3.1 \pm 0.1$.

$\Longrightarrow A_\mathrm{V}$ known if $E(\mathrm{B}-\mathrm{V})$ known!

Note also that $A_\mathrm{V}/E(\mathrm{B}-\mathrm{V}) \propto r$ since $\tau = n\sigma_{\mathrm{scat}} r$

$\Longrightarrow$ can measure distance! Generally, $A_\mathrm{V} \sim 1\ldots2\,\mathrm{mag\,pc}^{-1}$.

Extinction, V

The normalized reddening observed is roughly $\propto 1/\lambda$.

Explanation: scattering of radiation on grains.

The overall theory is very complicated, so only show the rough idea here...

In scattering, intensity is

$$I = I_0 \exp(-n\pi a^2 Q l) \tag{3.42}$$

where the quality factor Q has two components:

$$Q = Q_{\text{abs}} + Q_{\text{sca}} \tag{3.43}$$

Q_{abs}: absorption,

Q_{sca}: scattering.

(see next slide)

Note that Q is proportional to the optical depth...

Define the Albedo of particles

$$\gamma = \frac{Q_{\text{sca}}}{Q_{\text{abs}} + Q_{\text{sca}}} \tag{3.44}$$

(note that in principle there is also an angular dependence)

Extinction, VI

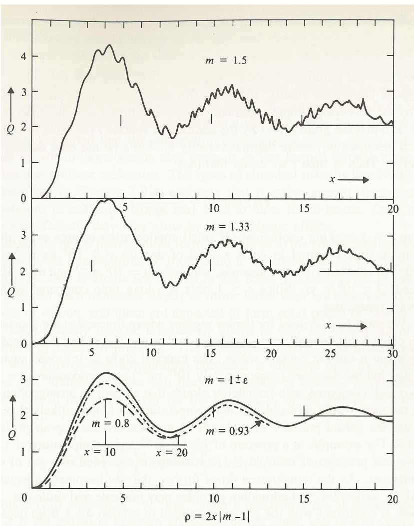

4.5. Extinction curves for spheres computed from Mie's formula for m =

Detailed theory: Mie scattering; gives $Q \propto 1/\lambda$ for small diameters $a \Longrightarrow$ as observed!

Q_{sca} as a function of $x = 2\pi a/\lambda$ for several dielectric constants m (Dyson& Williams, Fig. 4.5; $m = 1.33$ is water ice)

Extinction, VII

For detailed theory also need size distribution of grains.

Common assumption:

$$n(a) = Aa^{-3.5} \tag{3.45}$$

("MRN distribution"; Mathis, Rumpl, Nordsieck; 0.005 μm $< a <$ 0.25 μm) determined from fitting extinction curves.

Overall $1/\lambda$-behavior is understood as being due to Mie scattering

2200 Å feature:

- graphite grains? Optical constants change dramatically around 2200 Å for small graphite grains.
- Silicate grains?
- Polycyclic aromatic hydrocarbons (PAHs)?

Dust Models

Major dust models:

- MRN model
- Core-mantle models
- post-IRAS models

Models must take constraints on dust models into account:

- extinction curve (IR to UV)
- abundance deficiency of ISM gas phase
- (narrow) spectral features

See Witt, IAU Symp. 197, for a discussion of results.

UIBs

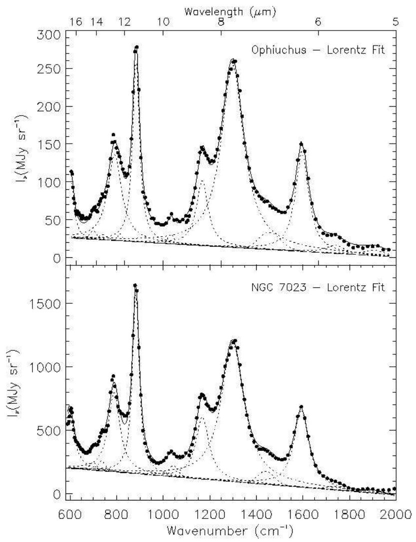

Unidentified emission structures seen at 3.3, 6.2, 7.7, 8.6, 11.3 μm seen in H II regions, YSOs, diffuse ISM, and even AGN: "unidentified infrared bands"

(Boulanger et al.; 1998)

PAHs, I

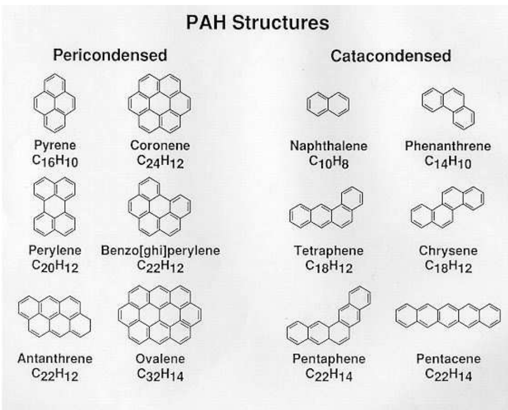

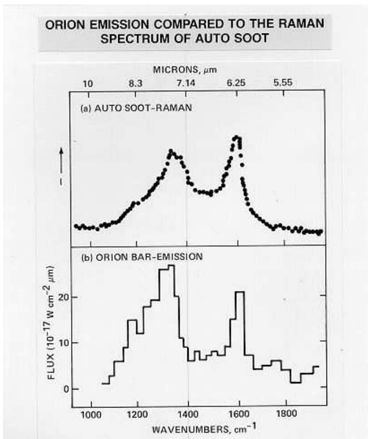

UIB emission is probably due to polycyclic aromatic hydrocarbons (PAHs), complex large carbonaceous molecules (UIB: related to C-C, C-H modes)

PAHs, II

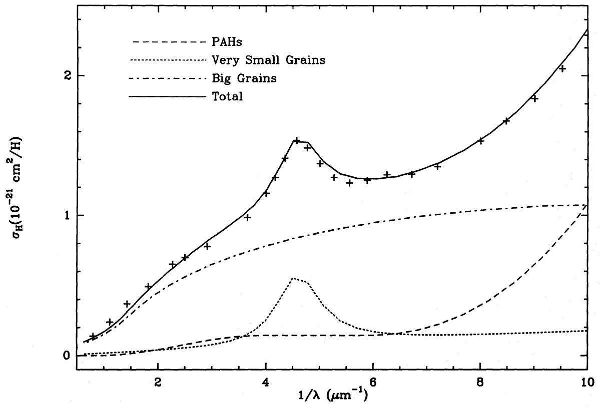

Inclusion of PAHs in dust models can also account for extinction curve, need three distinct populations:

- big grains (15 nm to 110 nm),
- very small grains (1.2 nm to 15 nm)
- PAHs (<1.2 nm)

Also predicts UIB emission!

Dśert, Boulanger, Puget (1990)

A problem with the Désert et al. model is the small size of large grains, which is inconsistent with X-ray halos. . . Possible solution: fluffy grains (Fogel & Leung, 1998)

Dust Formation

Where does dust come from?

Three potential sources:

1. Condensation out of the ISM
2. Condensation in cool stellar outflows
3. Condensation in protostars

ad 1) only possible in very dense molecular clouds: formation of clusters of 10. . . 20 atoms as "condensation nuclei"; accretion of further molecules via collisions.

Due to small densities dust formation timescale very long (10^8 years), thus rather impossible.

Dust is mainly generated in stars and then ejected into the ISM.

Dust Formation

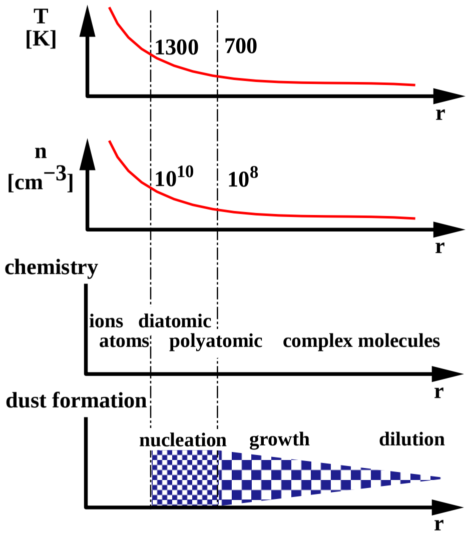

Dust formation in stars

Stellar atmospheres have much higher density than GMCs (solar photosphere: $10^{17}\,\mathrm{cm}^{-3}$, late type giants: $\sim 10^{15}\,\mathrm{cm}^{-3}$, compared to $10^{6}\,\mathrm{cm}^{-3}$ in GMCs)

$\Longrightarrow$ much higher condensation probability.

General process:

1. formation of molecules
2. accretion of more material, formation of clusters
3. formation of macroscopic particles

(Sedlmayr & Krüger; 1997)

Dust Formation

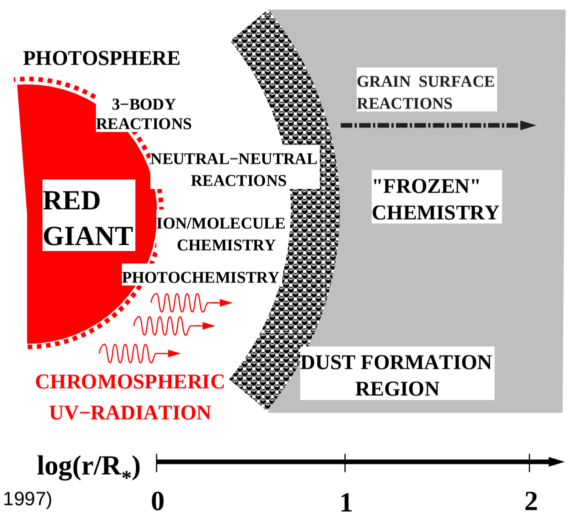

(Sedlmayr & Krüger; 1997)

Complex nonstationary chemistry makes things very complicated. . .

Dust Formation

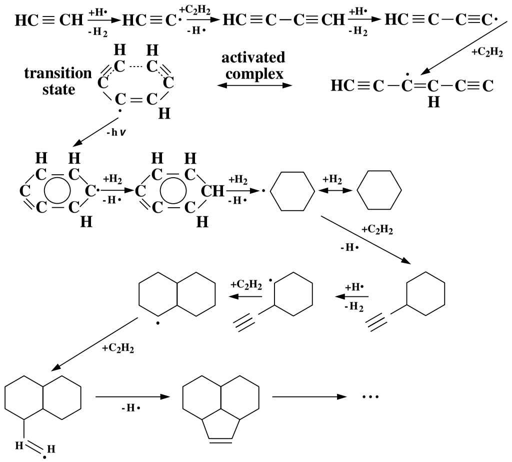

(Sedlmayr & Krüger; 1997)

Possible chemical reaction network for generation of PAHs in C-stars.

Introduction

Once gas and dust coalesce: formation of stars

Stars synthese higher elements out of H, He, and whatever metals they were formed from, and partly eject them back into ISM

$\Longrightarrow$ Elemental abundances change

$\Longrightarrow$ Galactic chemical evolution

In contrast to previous section, now “chemistry” really means “elemental abundances”.

We will use Galaxy as example, since it is the best studied object, and then come back to what different spirals do later.

Background information: Prantzos (2008) and Pagel (2009)

Closed Box Model, I

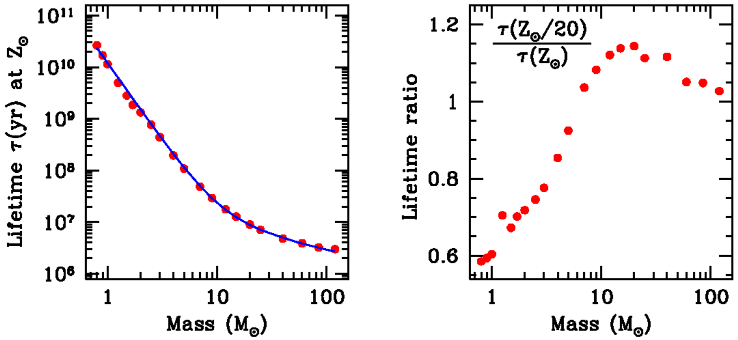

(Prantzos, 2008, Fig. 1)

Galactic metallicity evolution is influenced by:

- stellar formation rates
- stellar evolution and stellar death rates (which depend on metallicity!)

Closed Box Model, II

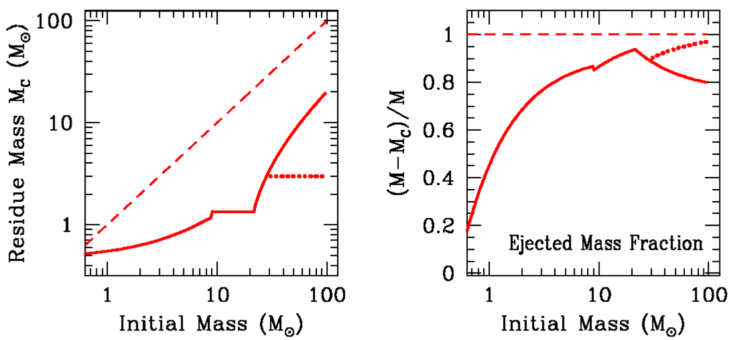

(Prantzos, 2008, Fig. 2)

Galactic metallicity evolution is influenced by:

- stellar mass ejection rates

Closed Box Model, III

Galactic metallicity evolution is influenced by:

- stellar evolution (see previous slides)
- inflow from outside galaxy
- ejection from galaxy
- mixing of elements within galaxy (influences populations).

Will look here at a simple model: one-zone, instantaneous recycling:

- gas well mixed
- stars return fusion products immediately
- no gas escapes/added (closed-box model)

Closed Box Model, IV

Let

- $M_{\mathrm{g}}(t)$: Mass of gas in galaxy at time t
- $M_{\mathrm{s}}(t)$: Mass in low-mass stars and compact objects (i.e., mass locked in stellar objects throughout lifetime of Galaxy)
- $M_{\mathrm{h}}(t)$: Mass of metals ($Z > 2$) in galactic gas.

Then the Metal abundance is

$$Z(t) = \frac{M_{\mathrm{h}}(t)}{M_{\mathrm{g}}(t)} \tag{3.46}$$

Stellar lifetimes:

- $Z = Z_\odot$, $M = M_\odot \Longrightarrow \tau \sim 11.4$ Gyr,
- $Z = Z_\odot$, $M = 0.8\,M_\odot$: $\Longrightarrow \tau \sim 23$ Gyr,
- $Z = 0.05 Z_\odot$, $M = 0.8\,M_\odot$: $\Longrightarrow \tau \sim 13.8$ Gyr

Stars with $M = 0.8\,M_\odot$: lowest mass stars that have ever died (=heaviest stars surviving in oldest globular clusters).

Closed Box Model, V

Assume formation of massive stars which produce metals. Let

- ΔM_s: mass in remnants
- $p \cdot \Delta M_s$: mass returned to ISM (p: yield, depends on initial mass function and evolution)
- $Z \cdot \Delta M_s$: metals locked in remnants

$\Longrightarrow$ change in mass of metals due to formation of stars given by

$$\Delta M_h = p \cdot \Delta M_s - Z \cdot \Delta M_s = (p - Z)\Delta M_s \tag{3.47}$$

(assuming instantaneous recycling)

$\Longrightarrow$ metallicity increases by

$$\Delta Z = \Delta\left(\frac{M_h}{M_s}\right) = \frac{p \cdot \Delta M_s - Z\,(\Delta M_s + \Delta M_g)}{M_g} \tag{3.48}$$

where $-Z \cdot \Delta M_g$ term due to exchange of mass with other regions.

Note that in the closed box case (no gas enters/leaves the system):

$$\Delta M_s = -\Delta M_g \tag{3.49}$$

Closed Box Model, VI

Define as primary elements those elements for which the formation is independent of Z (i.e., p independent of Z).

For these elements and a closed box ($\Delta M_s = -\Delta M_g$):

$$\Delta Z = \frac{p \cdot \Delta M_s - Z\,(\Delta M_s + \Delta M_g)}{M_g} = -p\frac{\Delta M_g}{M_g} \quad \Longrightarrow \quad \frac{dZ}{dt} = -\frac{p}{M_g}\frac{dM_g}{dt} \tag{3.50}$$

such that

$$\int_0^t \frac{dZ}{dt}\,dt = -p\int_{M(t=0)}^{M(t)} \frac{dM_g}{M_g} = -p\ln\frac{M_g(t)}{M_g(t=0)} \tag{3.51}$$

and finally

$$Z(t) = Z(t=0) + \ln\frac{M_g(t=0)}{M_g(t)} \tag{3.52}$$

Note that $M_g(t) < M_g(t=0)$, and therefore $\ln M_g(0)/M_g(t) > 0$, such that

- $Z(t)$ increases with time, and
- $Z(t)$ is higher in regions with less gas.

Closed Box Model, VII

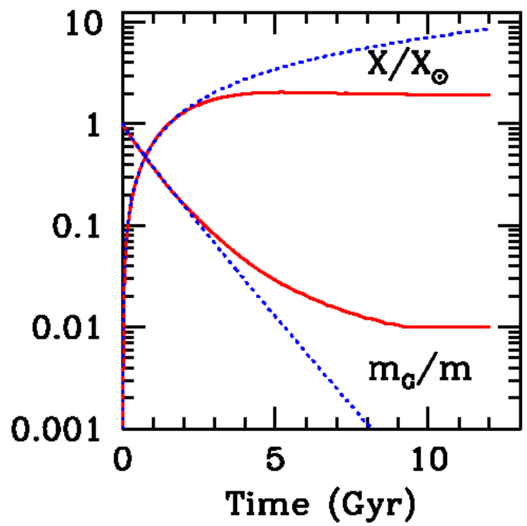

Evolution of abundance, X, and gas fraction, m_G, with time.

Calculations for closed box model in Instantaneous Recycling Approximation (IRA) and Non-IRA (stellar evolution)

(Prantzos, 2008, Fig. 12)

Closed Box Model, VIII

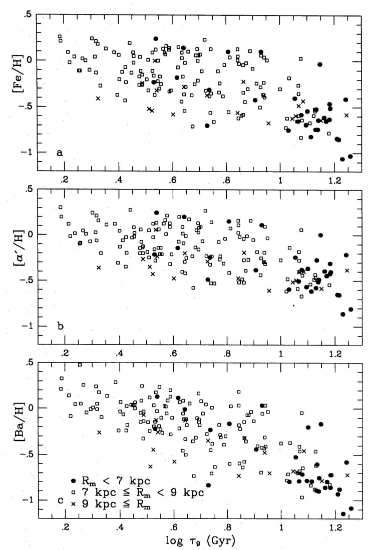

Younger stars in solar vicinity tend to be richer in metals.

Notation used:

$$[\text{Fe/H}] = \log_{10}\frac{A_{Fe}/A_H}{A_{Fe,\odot}/A_{H,\odot}} \tag{3.53}$$

where

- A_i: abundance by number of element i, and
- $A_{i,\odot}$: solar abundance by number of element i.

α: α-process elements (esp. Mg, Si, Ca, Ti)

Edvardsson et al. (1993, Fig. 14)

Closed Box Model, IX

We had

$$Z(t) = Z(t=0) + \ln\frac{M_g(t=0)}{M_g(t)} \qquad (3.52)$$

But the mass in low-mass stars formed before time t is

$$M_s(t) = M_g(t=0) - M_g(t) \qquad (3.54)$$

But these stars have lower metallicity. Therefore the mass in low metallicity stars is

$$M_s(Z < Z(t)) = M_g(t=0)\left(1 - \exp\left\{-\frac{Z(t)-Z(t=0)}{p}\right\}\right) \qquad (3.55)$$

Where the gas density is high vs. number of stars, the average metallicity must be low.

This effect is seen, e.g., in Large Magellanic Cloud or as metal abundance gradient in spirals.

Closed Box Model, X

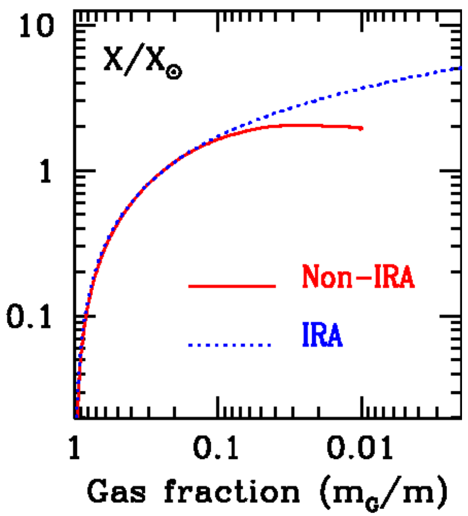

Abundance as function of gas fraction in the closed box model in Instantaneous Recycling Approximation (IRA) and Non-IRA (stellar evolution).

(Prantzos, 2008, Fig. 12)

Closed Box Model, XI

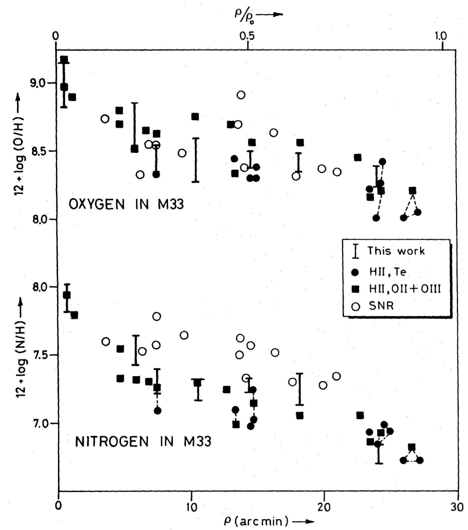

(Vilchez et al., 1988, Fig. 9)

Spiral galaxies generally show abundance gradients away from their core, as predicted by closed box models.

Closed Box Model, XII

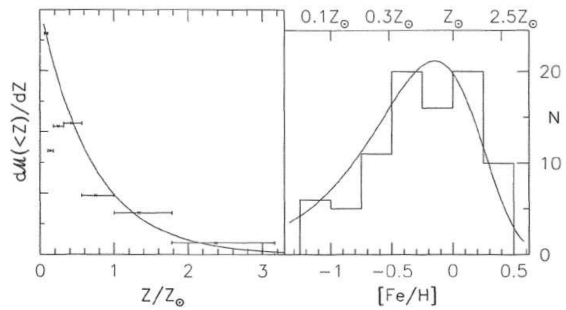

(Metallicity for "Baade's Window"; SG, Fig. 4.16)

The metallicity in low-mass stars was

$$M_s(<Z) = M_{g,0}\left(1 - e^{-\frac{Z(t)-Z_0}{p}}\right) \qquad (3.55)$$

and once all gas is gone, the mass of stars with metallicity in $[Z, Z+\Delta Z]$:

$$\frac{dM_s(<Z)}{dZ}\Delta Z \propto \exp\left(-\frac{Z(t)-Z(t=0)}{p}\right)\Delta Z \qquad (3.56)$$

This reproduces well the metallicity distribution found in the galactic bulge (see figure), and one finds $p \sim 0.7 Z_\odot$.

Bulge seems to have managed to convert all of its gas into stars!

3–86

Problems of Closed Box

Dwarf spheroidal galaxy Leo I (next to Regulus)

1. loss of metals?
   $\Longrightarrow$ galaxies have low mass, thus escape velocity is low

(2nd explanation is preferred)

For other regions, closed box is clearly wrong

Dwarf spheroidal galaxies: very little gas, but metallicity still low.
Two explanations:

1. Possibly low formation of massive stars (=different Initial Mass Function)
   $\Longrightarrow$ little formation of metals?

3–87

Solar Neighborhood

Surface density $\Sigma = \int_{-\infty}^{+\infty} n d\ell$ of stuff in solar neighborhood:

- stellar density: $\Sigma =$ 30–40 $M_\odot$ pc^{-2} (30 $M_\odot$ pc^{-2} in stars, 8 $M_\odot$ pc^{-2} in stellar residues)
- gas density: $\Sigma =$ 13 $M_\odot$ pc^{-2}

so total surface density is 50 $M_\odot$ pc^{-2}.

n: mass density ($M_\odot$ pc^{-3})

In neighborhood, abundance is $0.7Z_\odot$ (i.e., Sun is enriched!). Therefore

$$Z(\text{now}) = 0.7Z_\odot = p\ln(50/13) \quad \Longrightarrow \quad p \sim 0.5Z_\odot \tag{3.57}$$

this is slightly lower than bulge ($p \sim 0.7Z_\odot$), but could be explained if disk is less efficient in retaining gas (galactic fountain!).

However, further problem: predicted fraction of metal poor stars

$$\frac{M_\text{s}(Z < 0.25Z_\odot)}{M_\text{s}(Z < 0.7Z_\odot)} = \frac{1 - \exp(-Z_\odot/4p)}{1 - \exp(-0.7Z_\odot/p)} \sim 0.52 \tag{3.58}$$

so 50% of all stars in vicinity should have low abundances.

Reality: <20% of all stars have $Z < 0.25Z_\odot$: G-dwarf problem

Possible solution: local region was enriched by Supernovae to $Z(0) \sim 0.15Z_\odot$.

Bekki K., Chiba M., 2009, Proc. Astron. Soc. Aust. 26, 48

Edvardsson B., Andersen J., Gustafsson B., et al., 1993, A&A 275, 101

Gordon K.D., Bailin J., Engelbracht C.W., et al., 2006, ApJ 638, L87

Kim S., Staveley-Smith L., Dopita M.A., et al., 1998, ApJ 503, 674

Mateo M.L., 1998, ARA&A 36, 435

Mathewson D.S., Cleary M.N., Murray J.D., 1974, ApJ 190, 291

Meixner M., Gordon K.D., Indebetouw R., et al., 2006, AJ 132, 2268

Pagel B.E.J., 2009, Nucleosynthesis and Chemical Evolution of Galaxies, CUP, Cambridge, 2nd edition

Prantzos N., 2008, In: C. Charbonnel & J.-P. Zahn (ed.) Stellar Nucleosynthesis: 50 years after B2FH, Vol. 32. EAS Publ. Ser., p.311

Putman M.E., Staveley-Smith L., Freeman K.C., et al., 2003, ApJ 586, 170

Solomon P.M., Rivolo A.R., 1989, ApJ 339, 919

Solomon P.M., Rivolo A.R., Barrett J., Yahil A., 1987, ApJ 319, 730

Vilchez J.M., Pagel B.E.J., Diaz A.I., et al., 1988, MNRAS 235, 633